

Free energy inference from partial work measurements in small systems

M. Ribezzi-Crivellari

Departament de Física Fonamental,
Universitat de Barcelona,
Diagonal 647, 08028 Barcelona, Spain

and

F. Ritort

Departament de Física Fonamental,
Universitat de Barcelona,
Diagonal 647, 08028 Barcelona, Spain

Ciber-BBN de Bioingeniería, Biomateriales y Nanomedicina,
Instituto de Salud Carlos III,
Madrid, Spain

Abstract

Fluctuation relations (FRs) are among the few existing general results in non-equilibrium systems. Their verification requires the measurement of the total work (or entropy production) performed on a system. Nevertheless in many cases only a partial measurement of the work is possible. Here we consider FRs in dual-trap optical tweezers where two different forces (one per trap) are measured. With this setup we perform pulling experiments on single molecules by moving one trap relative to the other. We demonstrate that work should be measured using the force exerted by the trap that is moved. The force that is measured in the trap at rest fails to provide the full dissipation in the system leading to a (incorrect) work definition that does not satisfy the FR. The implications to single-molecule experiments and free energy measurements are discussed. In the case of symmetric setups a new work definition, based on differential force measurements, is introduced. This definition is best suited to measure free energies as it shows faster convergence of estimators. We discuss measurements using the (incorrect) work definition as an example of partial work measurement. We show how to infer the full work distribution from the partial one via the FR. The inference process does also yield quantitative information, e.g. the hydrodynamic drag on the dumbbell. Results are also obtained for asymmetric dual-trap setups. We suggest that this kind of inference could represent a new and general application of FRs to extract information about irreversible processes in small systems.

Significance Statement

Fluctuation Relations (FRs) provide general results about the full work (or entropy production) distributions in non-equilibrium systems. However, in many cases the full work is not measurable and only partial work measurements are possible. The latter do not fulfill a FR and cannot be used to extract free energy differences from irreversible work measurements. We propose a new application of FRs to infer the full work distribution from partial work measurements. We prove this new type of inference using dual-trap optical tweezers where two forces (one per trap) are measured, allowing us to derive full and partial work distributions. We derive a set of results of direct interest to single molecule scientists and, more in general, to physicists and biophysicists.

Introduction

Fluctuation Relations (FRs) are mathematical equations connecting non equilibrium work measurements to equilibrium free energy differences. FRs, such as the Jarzynski Equality (JE) or the Crooks Fluctuation Relation (CFR) have become a valuable tool in single-molecule biophysics where they are used to measure folding free energies from irreversible pulling experiments [1, 2]. Such measurements have been carried out with laser optical tweezers on different nucleic acid structures such as hairpins [3, 4, 5, 6], G-quadruplexes [7, 8] and proteins [9, 10, 11, 12], and with Atomic Force Microscopes on proteins [13] and bi-molecular complexes [14]. An important issue regarding FRs is the correct definition of work, which rests on the correct identification of configurational variables and control parameters. In the single-trap optical tweezers configuration this issue has been thoroughly discussed [17, 18, 19].

The situation about how to correctly measure work in small systems becomes subtle when there are different forces applied to the system. In this case theory gives the prescription to correctly define the work (W_Γ) for a given trajectory (Γ): integrate the generalized force (f_λ) (conjugated to the control parameter, λ) over λ along Γ , $W_\Gamma = \int_\Gamma f_\lambda d\lambda$. However, in some cases one cannot measure the proper generalized force or has limited experimental access to partial sources of the entropy production leading to what we call incorrect or partial work measurements. A remarkable example of this situation are dual-trap setups, mostly used as the high-resolution tool for single molecule studies (Fig. 1A). In this case a dumbbell formed by a molecule tethered between two optically trapped beads is manipulated by moving one trap relative to the other. In this setup two different forces (one per trap) can be measured and at least two different work definitions are possible. In equilibrium conditions, i.e. when the traps are not moved both forces are equivalent: the forces acting on each bead have equal magnitude and opposite sign. On the contrary, in pulling experiments, where one trap is at rest (with respect to water) while the other is moved, the two forces become inequivalent. This is so because the center of mass of the dumbbell drifts and the beads are affected by different viscous drags (purple arrows in Fig. 1B). In such conditions theory prescribes that the full thermodynamic work must be defined on the force measured at the moving trap whereas the force measured in the trap at rest (with respect to water) leads to a *partial work measurement* which, as we show below, entails a systematic error in free

energy estimates. The difference between both works equals the dissipation by the center of mass of the dumbbell, which is only correctly accounted for in the correct work definition.

In this paper we combine theory and experiments in a dual-trap setup to demonstrate several results. First, we show that if the wrong work definition is used, free energy estimates will be flawed. The error is especially severe in the case of unidirectional work estimates (e.g. JE) while it influences bi-directional estimates to a lesser extent. This fact is not purely academical: measuring the force in the trap at rest is experimentally easier in dual-trap setups and, in fact, many groups choose to do so [5, 20, 21]. For example if different lasers are used for trapping and detection, measuring the force in the moving trap poses the additional challenge of keeping the trapping and detection lasers aligned while moving them. Second, we show how it is possible, by using the CFR, to *infer* the full work distribution from partial work measurements. We demonstrate this new type of inference in our dual-trap setup by showing how to reconstruct the correct work distribution (i.e the one we would have measured in the moving optical trap) from partial work measurements in the wrong optical trap (i.e. the one at rest with respect to water) by using the CFR. In particular, for symmetric setups the correct work distribution can be directly inferred by simply shifting the partial work distribution. In asymmetric setups inference is still possible in the framework of a Gaussian approximation, but the knowledge of some equilibrium properties of the system is still required. This type of inference should be seen as an example of a more general application of FRs which aims at extracting information about the total entropy production of a nonequilibrium system from partial entropy production measurements. This allows us to determine the average power dissipated by the center of mass of the dumbbell, from which we can extract the corresponding hydrodynamic coefficient thereby avoiding direct hydrodynamic measurements. Moreover, we argue this type of inference might find applicability to future biophysical experiments where the sources of entropy production are not directly measurable, e.g. ATP-dependent motor translocation where the hydrolysis reaction cycle cannot be followed one ATP at a time. Finally we show how, in symmetric setups, the work definition satisfying the CFR is not unique. In particular the *differential work*, based on differential force measurements [22], still satisfies the CFR and leads to the least biased free energy estimates. The distinguishing feature of this work definition is that it completely filters out the dissipation due to the motion of the center of mass of the dumbbell.

Throughout the paper, and for simplicity and pedagogical reasons, most of the derivations, calculations and experiments are shown for symmetric dual-trap setups whereas the asymmetric case is discussed towards the end of the paper.

The model

In dual-trap setups a molecule is stretched by two optical traps, the control parameter λ being the trap-to-trap distance. Let A,B denote the two optical traps. When one trap (say trap A) is moved with respect to the bath while trap B is at rest, suitable configurational variables are the positions of the beads, both measured from the center of the trap at rest (trap B). We shall denote these variables by y_A and y_B , Fig. 1B. The total energy of the system is composed of three terms:

$$U(y_A, y_B, \lambda) = U_m(y_A - y_B) + \frac{k_B}{2} y_B^2 + \frac{k_A}{2} (\lambda - y_A)^2, \quad (1)$$

where the quadratic terms model the potential of the optical trap and U_m describes the properties of the tether. However one could measure the positions of the beads and the trap-to-trap distance in the moving frame of trap A (x_A , x_B and $-\lambda$ in Fig. 1B), and the potential energy in Eq. (1) would be written as:

$$U'(x_A, x_B, \lambda) = U_m(x_A - x_B) + \frac{k_A}{2} x_A^2 + \frac{k_B}{2} (\lambda + x_B)^2, \quad (2)$$

where $y_A - x_A = y_B - x_B = \lambda$ (x_A and x_B are negative). Central to our analysis will be the equation connecting the potential U and the work performed on the system by changing the control parameter [1]:

$$W = \int_{t_i}^{t_f} dt \partial_t U. \quad (3)$$

From Eq. (1) we get:

$$W = \int_{t_i}^{t_f} f_A \dot{\lambda} dt, \quad (4)$$

with $f_A = -k_A(y_A - \lambda)$. Inserting U' instead of U in (3) gives:

$$W' = \int_{t_i}^{t_f} dt \partial_t U' = - \int_{t_i}^{t_f} f_B \dot{\lambda} dt, \quad (5)$$

Despite of their similarity we will show that W and W' are remarkably different. In fact, from the reference frame of trap A, the bath is seen to flow with velocity $-\dot{\lambda}$ (Fig. 1B). Because of this flow an experiment in which trap A is moved is not Galilean equivalent to one in which trap B is moved. In the presence of a flow the connection between potential and work, Eq. (3), is not valid anymore. In fact thermodynamic work measurements must be based on the force measured in the trap being moved. This fact has been discussed in [23], yet the implications to single-molecule experiments have never been pointed out. Summarizing, if trap A is moved and B is at rest with respect to water, using the work W (Eq. (4)) in the JE leads to correct free energy estimates whereas using W' (Eq. (5)) in the JE leads to a systematic error. Below we quantify such error in detail. The difference between W and W' can be readily discussed in symmetric setups ($k_A = k_B = k$) where calculations are much simpler. To do this we switch to a new coordinate system: $x_+ = \frac{1}{2}(y_A + y_B)$, $x_- = y_A - y_B$. Here x_+ is the position of the geometric center of the dumbbell, while x_- is the differential coordinate [22]. In this coordinate system the potential Eq. (1) reads $U(x_-, x_+; \lambda) = U^-(x_-; \lambda) + U^+(x_+; \lambda)$:

$$\begin{aligned} U^-(x_-, \lambda) &= U_m(x_-) + \frac{k}{4}(x_- - \lambda)^2, \\ U^+(x_+, \lambda) &= k \left(x_+ - \frac{\lambda}{2} \right)^2. \end{aligned} \tag{6}$$

The potential energy term U_+ associated to x_+ is that of a moving trap, a problem that has been addressed both with experiments and theory [24, 25], while the potential energy term U_- associated to x_- corresponds to pulling experiments performed using a single trap and a fixed point. The dumbbell is in contact with an isothermal bath where the equilibrium state is described by the Boltzmann distribution and the corresponding partition function (we assume a weak system-environment coupling, a situation satisfied in our experimental conditions, Section S2 in the SI). Consequently, the two degrees of freedom are uncoupled and the total partition function for the system factorizes:

$$\begin{aligned} Z(\lambda) &= Z^+(\lambda)Z^-(\lambda) \\ Z^\pm(\lambda) &= \int dx_\pm \exp(-\beta U^\pm) \quad , \end{aligned} \tag{7}$$

with $\beta = (K_B T)^{-1}$, T being the temperature and K_B being Boltzmann constant. As a consequence free energy changes in the system can be decomposed into two contributions:

$$\Delta G = \Delta G^+ + \Delta G^-, \quad \Delta G^\pm = -\beta^{-1} \log Z^\pm. \quad (8)$$

Work can also be decomposed into two contributions, each regarding one of the subsystems: $W^\pm = \int \partial_t U^\pm(x_\pm; \lambda) dt$. Here W^- contains the work done in stretching the molecule while W^+ is pure dissipation due to the movement of the center of mass of the dumbbell. Note that:

$$W = W^- + W^+, \quad W' = W^- - W^+, \quad (9)$$

which shows that the difference between W and W' is entirely due to W^+ . The JE holds for W , the standard work definition, so that

$$\Delta G = -\beta^{-1} \log \langle \exp(-\beta W) \rangle. \quad (10)$$

Inserting Eqs. (8),(9) in (10) we get: $\Delta G^+ + \Delta G^- = -\beta^{-1} \langle \exp(-\beta (W^+ + W^-)) \rangle$. In symmetric setups W^+ and W^- are independently distributed random variables (see Sections S1 and S3 in the SI) and we can conclude that:

$$\Delta G^\pm = -\beta^{-1} \log \langle e^{-\beta W^\pm} \rangle. \quad (11)$$

Using the JE on both W and W' we get two different free energy estimates: ΔG (Eq. (10)) and $\Delta G' = -\beta^{-1} \log \langle \exp(-\beta W') \rangle$. The error \mathcal{E} committed by using W' instead of W can be quantified as:

$$\mathcal{E} = \Delta G - \Delta G' = -\beta^{-1} \log \frac{\langle \exp(-\beta W) \rangle}{\langle \exp(-\beta W') \rangle}. \quad (12)$$

From Eqs. (9),(10) and again using the fact W^+ and W^- are independently distributed random variables we get $\langle \exp(-\beta W) \rangle = \langle \exp(-\beta (W^+ + W^-)) \rangle = \langle \exp(-\beta W^+) \rangle \langle \exp(-\beta W^-) \rangle$ and similarly for W' . As a consequence $\frac{\langle \exp(-\beta W) \rangle}{\langle \exp(-\beta W') \rangle} = \frac{\langle \exp(-\beta W^+) \rangle}{\langle \exp(+\beta W^+) \rangle}$ and Eq. (12) is reduced to

$$\mathcal{E} = -\beta^{-1} \log \frac{\langle \exp(-\beta W^+) \rangle}{\langle \exp(+\beta W^+) \rangle}. \quad (13)$$

Since x_+ is subject to a quadratic potential (Eq. (6)), we expect W^+ to be a Gaussian random variable. This is not true in general for W^- given that x_- feels the nonlinear term U_m . For Gaussian Random Variables we have:

$$\beta^{-1} \log \langle \exp(\pm \beta W^+) \rangle = \langle W^+ \rangle \pm \frac{\beta}{2} \sigma_+^2, \quad (14)$$

where by σ_+^2 we denote the variance of W^+ . Moreover dragging a trapped bead in a fluid causes no free energy change, so that:

$$\Delta G^+ = -\beta^{-1} \log \langle \exp(-\beta W^+) \rangle = \langle W^+ \rangle - \frac{\beta}{2} \sigma_+^2 = 0 \quad (15)$$

or $\langle W^+ \rangle = \frac{\beta}{2} \sigma_+^2$. Inserting Eqs. (14) and (15) in Eq. (13) we get:

$$\mathcal{E} = \langle W^+ \rangle + \frac{\beta}{2} \sigma_+^2 = 2\langle W^+ \rangle. \quad (16)$$

Equation (16) gives $\mathcal{E} = \beta \sigma_+^2 > 0$ showing that $\Delta G'$ is lower than ΔG (Eq. (12)). Interestingly enough, using W' instead of W in the JE leads to free energy estimates in apparent violation of the second law. The error on free energy estimates obtained using W' instead of W is proportional to the mean work performed on the center of the dumbbell. This mean work $\langle W^+ \rangle$ is just the mean friction force times the total trap displacement $\Delta\lambda$:

$$\langle W^+ \rangle = \gamma_+ \frac{\dot{\lambda}}{2} \Delta\lambda, \quad (17)$$

where γ_+ is the friction coefficient of the drag force opposing the movement of the geometric center of the dumbbell. The value of γ_+ can be independently obtained from equilibrium measurements [26] (Sections S4,S5 in the SI).

Differential Work Measurements

Equations (9) and (15) show that free energy estimates based on the standard work W and the differential work W^- are equivalent:

$$\begin{aligned} \Delta G &= -\beta^{-1} \log \langle \exp(-\beta W) \rangle = \\ &= -\beta^{-1} \log \langle \exp(-\beta W^-) \rangle - \beta^{-1} \log \langle \exp(-\beta W^+) \rangle = \\ &= -\beta^{-1} \log \langle \exp(-\beta W^-) \rangle = \Delta G^-. \end{aligned} \quad (18)$$

We stress that this is only true for symmetric setups where W^+ and W^- are independent random variables. The case of asymmetric setups is discussed further below. Therefore W^- can be used for free energy determination, as it has been done in [11], although without discussion. Equation (18) does only hold when the number of work measurements, N , tends to infinity. In all practical cases we deal with finite N and the Jarzynski estimator is biased [27, 28]. The bias is strongly linked to the typical dissipation D_{typ} and a reliable estimate of free energy differences requires a number of work measurements which scales as $N \simeq \exp(D_{\text{typ}})$ [29, 30], so that even a small reduction in D_{typ} entails a considerable improvement in the convergence of free energy estimators. Moreover the bias is superadditive. Let us consider for simplicity Gaussian Work Distributions. In this case the bias, B_N^{GWD} , in the large N limit is a function of the variance of the distribution σ^2 and of N [27]:

$$B_N^{\text{GWD}} = \frac{\exp(\beta^2 \sigma^2 - 1)}{2\beta N} . \quad (19)$$

B_N^{GWD} is a convex function of σ , and is superadditive i.e. $B_N^{\text{GWD}}(\sigma^2 + \phi^2) > B_N^{\text{GWD}}(\sigma^2) + B_N^{\text{GWD}}(\phi^2)$. This means that, should the work be the sum of two independent Gaussian contributions, the bias on the sum is greater than the sum of the biases. Although Eq. (19) was derived under strong assumptions, superadditivity does also hold for other theoretical expressions for the bias and has been checked in our experimental data (see below). Let us introduce the following Jarzynski estimators for finite N :

$$\Delta G_N = -\beta^{-1} \log \frac{1}{N} \sum_{i=1}^N e^{-\beta W_i}, \quad (20)$$

$$\Delta G_N^\pm = -\beta^{-1} \log \frac{1}{N} \sum_{i=1}^N e^{-\beta W_i^\pm} \quad (21)$$

and the corresponding bias functions:

$$B_N = \Delta G_N - \Delta G \quad (22)$$

$$B_N^\pm = \Delta G_N^\pm - \Delta G. \quad (23)$$

Since $W = W^+ + W^-$, superadditivity guarantees:

$$B_N \geq B_N^- + B_N^+ \geq B_N^-. \quad (24)$$

Because of Eq. (24) differential work measurements always improve the convergence of free energy estimates in dual-trap setups. This is especially important in all those cases in which bidirectional methods (e.g. the CFR) cannot be used and one has to employ unidirectional methods.

Pulling on ds-DNA

The theory discussed so far has been put to test in a series of pulling experiments performed in a recently developed dual-trap optical tweezers setup which directly measures force in each trap [31, 32]. The setup can move the two optical traps independently and measure their relative position with sub-nanometer accuracy, giving direct access to both W and W' . In these experiments 3 kb ds-DNA tethers ($\simeq 1 \mu\text{m}$ in contour length) were stretched between 1 and 3 pN (Fig. 1C) in a symmetric dual-trap setup ($k_A = k_B = 0.02\text{pN/nm}$) using $4 \mu\text{m}$ silica beads as force probes. The experiments were performed moving one of the two traps (trap A) with respect to the lab frame and leaving trap B at rest. All experiments were performed in PBS buffer (pH 7.4, 1M NaCl). We chose cyclical protocols ($\lambda_t : \lambda_0 = \lambda_{T_c}$, where T_c is the total duration of the cyclic protocol). The excursion of the control parameter, $\Delta\lambda = \lambda_{T_c/2} - \lambda_0$, was varied between 200, 400 and 600 nm, while the pulling speed was varied between 1.35 ± 0.05 , 4.3 ± 0.1 and $7.2 \pm 1 \mu\text{m/s}$. Given the force-distance curves the total dissipation along cycles was measured:

$$D = \oint d\lambda f_A, \quad D' = - \oint d\lambda f_B. \quad (25)$$

The CFR [16] is a symmetry relation between the work distribution associated to the forward (P_F) and time reversed (P_R) protocols:

$$P_F(W) = P_R(-W) \exp(\beta(W - \Delta G)). \quad (26)$$

In the case of cyclic protocols $P_F = P_R = P$ and $\Delta G = 0$ so that the CFR takes the form:

$$P(D) = \exp(\beta D) P(-D). \quad (27)$$

Such symmetry of the probability distribution for D can be directly tested in cases where negative dissipation events are observed. In Fig. 2A we show measured work histograms (solid points, left hand side of Eq. (27)) and reconstructed histograms (open points, right hand side of Eq. (27)). If Eq.

(27) is fulfilled then the measured and reconstructed histograms match each other. A quantitative measure of the deviation from Eq. (27) can be obtained from the ratio $P(D)/P(-D)$, as shown in Fig. 2B. Experimental data shows that D fulfills the FR whereas D' does not. In Fig. 2C we show that the pdfs of D^+ and D^- , with:

$$D^- = \frac{D + D'}{2} \quad (28)$$

$$D^+ = \frac{D - D'}{2}, \quad (29)$$

are experimentally found to satisfy a FR as in Eq. (27). D^- is just the differential work, W^- , Eq. (9) evaluated on a cyclic protocol, whereas D^+ is the dissipation due to the movement of the center of mass of the dumbbell. Summarizing, although in general W is the only observable we expect to fulfill a FR, in symmetric setups two new FRs emerge, for W^- and W^+ . In Fig. 3A,B we compare the predictions of Eqs. (12), (17) with experimental results for different pulling speeds, $\dot{\lambda}$, and different displacements $\Delta\lambda$. Equation (17) must be used to correct free energy estimates obtained in all those dual-trap setups which do not measure the force applied by the trap which is being moved (as in [5, 20, 21]). The advantages of using W^- in free energy estimates are shown in Fig. 3C. There we show the convergence of the Jarzynski estimator with sample size for the cycles in Fig. 1C. Being evaluated over cycles, the expected free energy change is zero. The convergence of the estimator is faster for W^- than for W in the three cases (Eq. (24)). The effect is enhanced in our experiments by the high pulling speed (in the range 1-7 μm) and by the large bead radius (2 μm). Let us note that due to the finite lifetime of molecular tethers and unavoidable drift effects, raising the pulling speed is a convenient strategy to improve the quality of free energy estimates. Similar results have been found also at low pulling speeds where, again, W' does not satisfy the CFR (Section S7 in the SI).

Experiments on DNA hairpins

Fluctuation theorems are used to extract folding free energies for nucleic acid secondary structures or proteins. We further tested the different work definitions by performing pulling experiments on a 20bp DNA hairpin (Fig. 4A) at a 0.96 ± 0.02 $\mu\text{m/s}$ pulling speed in the same dual-trap setup as in

the previous dsDNA experiments. In this case the work performed during the unfolding and refolding of the molecule were considered separately, as it is customary for free energy determination. In Fig. 4B we present forward and reverse work histograms for W, W' and W^+ . Again W and W^- both fulfill the CFR but W shows higher dissipation than W^- , resulting in slower convergence of unidirectional free energy estimators (Fig. 4C). The difference between unidirectional free energy estimates based on W and W^- is in this case $\simeq 1 K_B T$. As previously discussed for double-stranded DNA (Fig. 2A), W' does not fulfill the CFR and, as a consequence, unidirectional free energy estimates based on W' are flawed. In our experimental conditions the error committed by using the wrong work definition is again positive and equal to $\mathcal{E} \simeq 3 K_B T$. As previously discussed this leads to a negative average dissipated work, apparently violating the second law. It must be noted that the difference in free energy estimates based on W^- and W is a finite-size effect, whose magnitude decreases when an increasing number of work measurements is considered. On the contrary the error committed by using W' does not vanish by increasing the number of work measurements. It can be noted from Fig 4B that, although W' does not fulfill the CFR and gives wrong unidirectional estimates, its forward and reverse distributions apparently cross at $W' = \Delta G$ within the experimental error. Although this could be used for free energy determination the result should be taken with caution as we have no general proof that this should happen in all cases.

Free energy inference from partial work measurements

The JE and CFR are statements on the statistics of the total dissipation in irreversible thermodynamic transformations. The need to measure the total dissipation limits the range of applicability of these and other FRs. For example testing FRs concerning the dynamics of molecular motors would need the simultaneous measurement of both the work performed by the motor and the number of hydrolyzed ATPs. Here we demonstrate that, at least in some cases, a different approach is possible. Let us start by considering the simple case of symmetric setups as developed in the previous sections. In the experiments discussed so far there are two sources of dissipation that we were able to measure and characterize separately: the motion of the dumbbell

and the dissipation of the differential coordinate. We already learnt that W satisfies a FR while W' does not. Moreover we know that $W = (W_- + W_+)/2$ and $W' = (W_- - W_+)/2$, and that, being W^+ and W^- uncorrelated random variables, W and W' have the same variance. Imagine now to have only partial information on the system. For example, one could be able to measure force only in the trap at rest, as many experimental setups do. With this information, and in absence of any guiding principle, no statement about the total entropy production is possible. We will find such guiding principle if we assume the FR to hold for W . Knowing that W and W' have the same variance, we just have to shift the work distribution $P'(W')$ by $W = W' + \Delta$ to get a new distribution that satisfies the CFR. In practice this is done starting from the set of W' values and tuning the value of Δ (Fig. 5A) until $P(W) = P'(W - \Delta)$ fulfills the CFR (Fig. 5B). In the case of the hairpin, this same shifting procedure is operated for both forward and reverse work distributions. Again the value of Δ is tuned (Fig. 5C) until the CFR symmetry is recovered (Fig. 5D). The unique value of Δ that restores the validity of the CFR equals the average work dissipated by the motion of center of mass of the dumbbell, giving the hydrodynamic coefficient γ_+ via Eq. (17). Let us note that, once the work distribution in the correct trap (i.e. the moving trap) has been recovered, then we could also extract the correct free energy difference (the value of ΔG , Fig. 5E) and infer the distribution for the differential work W_- by deconvolution.

The extension of this analysis to the asymmetric case is more complex but equally interesting (Fig. 6A). The decomposition of W, W' in W^+ and W^- (Eq. (9)) is still possible although W^+, W^- are not uncorrelated variables anymore and neither W^+ nor W^- satisfy a FR. In this general case only W satisfies a FR (but not W', W^+, W^-). Remarkably enough, in the framework of a Gaussian approximation, it is still possible to infer the correct work distribution $P(W)$ out of partial work W' measurements. The analysis is presented in Section S6 of the SI. In this case it is enough to know the trap and molecular stiffnesses k_A, k_B, k_m i.e. some equilibrium properties of the system, for a successful inference. To reconstruct $P(W)$ both the mean and the variance of $P'(W')$ must be changed, which can be achieved by doing a convolution between the $P'(W')$ and a normal distribution: $P_{\Delta, \Sigma} = P' \star \mathcal{N}(\Delta, \Sigma)$ where \star denotes the convolution operator and $\mathcal{N}(\Delta, \Sigma)$ is a normal distribution with mean Δ and standard deviation Σ . Starting from a distribution $P'(W')$ there are infinitely many choices of Δ and Σ which yield a $P_{\Delta, \Sigma}(W)$ satisfying the CFR. Indeed, let us suppose that the pair

Δ^*, Σ^* is such that $P_{\Delta^*, \Sigma^*}(W)$ satisfies the CFR. Then it is easy to check that $P_{\Delta^* + \phi, \sqrt{\Sigma^{*2} + 2\phi K_B T}}$ will also satisfy the CFR for any ϕ (Fig. 6B). In this situation the inference cannot rest on the CFR alone. Explicit calculations in the Gaussian case (section S6 in SI) show that variances (σ^2) and means ($\langle \dots \rangle$) of $P(W)$ and $P'(W')$ are related by an Asymmetry Factor (AF),

$$AF(k_A, k_m, k_B) = \frac{\sigma_W^2 - \sigma_{W'}^2}{\langle W \rangle - \langle W' \rangle} = K_B T \frac{4k_m(k_A - k_B)}{k_A(k_B + 2k_m)} \quad (30)$$

which only depends on *equilibrium properties* such as the stiffnesses of the different elements (section S6.3 in the SI). Knowing the AF allows us to select the unique pair Δ, Σ such that $AF = \Sigma^2/\Delta$ with $P_{\Delta, \Sigma}(W)$ satisfying the CFR. The inference procedure can be described with a very simple formula (Section S6 in the SI). The key idea is to proceed as previously done in the case of symmetric setups by just shifting the mean of $P'(W')$ by a parameter δ until the CFR is satisfied, i.e. $\Delta = \delta, \Sigma = 0$. From the values of AF and δ we can reconstruct $P(W)$ by using the formulae,

$$\Delta = \frac{2\delta}{2 - \beta AF} ; \Sigma^2 = \frac{2\delta AF}{2 - \beta AF} \quad (31)$$

The inference procedure for an asymmetric setup is shown in Fig. 6C, 6D for cyclic ds-DNA pulling experiments. For non-cyclic pulls ($\Delta G \neq 0$) the procedure can be easily generalized in the line of what has been shown for the case of hairpin in the symmetric setup (Fig. 5C).

Discussion

FRs are among the few general exact results in non-equilibrium statistical mechanics. Their validity has been already extensively tested in different systems, ranging from single molecules to single electron transistors, and in different conditions (steady state dynamics, irreversible transformations between steady states, transient nonequilibrium states). At the present stage, the main widespread application of FR is free energy recovery from non-equilibrium pulling experiments in the single molecule field. What we are presenting here is a new application of FR for inference. All FRs are statements about the statistics of the total entropy production in a system plus the environment. If some part of the entropy production is missed or inadequately considered FRs will in general not hold. This is why, for irreversible

transformations between equilibrium states, we have a FR for the dissipated work (which is the total entropy production) but not for the dissipated heat (which is just the entropy production in the environment). The main tenet is now that the violation of FRs in a given setting provides useful information: it is an evidence that some contribution to the total entropy production is being missed. We have given rigorous examples in which the violation of FRs can be used to characterize the missing entropy production. Remarkably, in our model system, one could even replace the moving trap by a moving micropipette, an object lacking any measurement capability, and still infer the work distribution exerted by that object on the molecular system (this extremely asymmetric setup would still be described by Eq.(30), with $k_A \rightarrow \infty$ and $AF = 4K_B T k_m / (k_B + 2k_m)$). These results open the exciting prospect of extending and applying these ideas to steady state systems, such as molecular motors, to extract useful information about their mechanochemical cycle.

Conclusions

In order to give it a clear and definite meaning to free energy inference we have discussed irreversible transformations between equilibrium states performed with dual-trap optical tweezers. In these experiments a molecular tether is attached between two beads which are manipulated with two optical traps. The irreversible transformation is performed by increasing the trap-to-trap distance at a finite speed. In this kind of transformations the dissipated work equals the total entropy production leading to our first result: in pulling experiments work W must be defined on the force measured in the trap which is moved with respect to the thermal bath. The force measured in the trap at rest gives rise to a work definition, W' , which does not satisfy the FR and is unsuitable to extract free energy differences. We have called W' a partial work measurement because it misses part of the total dissipation. This result is of direct interest to experimentalists: many optical tweezers setups are designed so that they can only measure W' . We have thus imagined a situation in which W' is measurable while W is not and asked the question: can we infer the distribution of W from that of W' ? If the question is asked in full generality, without any system-specific information, the answer is probably negative. Knowing only the extent of violation of the FR will be of little use, in general some additional system specific information will be needed for a successful inference. Here we discussed free energy inference

in the framework of a Gaussian approximation, the extent to which such inference is generally possible should be the subject of future studies. Let us summarize our main results:

- A symmetry of the system can be crucial for the inference. For left-right symmetric systems (as exemplified in our symmetric dual-trap setup) the $P(W)$ can be inferred from $P'(W')$ just by imposing that the former satisfies the CFR. When symmetry considerations cannot be used, the knowledge of some equilibrium properties of the system may suffice to successfully guide the inference (such as the stiffnesses for the asymmetric setup).
- The inference process can be used both to recover the full dissipation spectrum plus additional information about the *hidden* entropy source. In our specific dual-trap example W' does not account for the dissipation due to the movement of the center-of-mass of the dumbbell and the inference procedure can be seen as a method to measure the associated hydrodynamic drag.
- We stress the benefits of using symmetric dumbbells in single molecule manipulation. In this case an alternative work definition, the *differential work* W^- , fulfills the CFR and is thus suitable for free energy measurements. Being W^- less influenced by dissipation than W , switching from W to W^- ensures faster convergence of unidirectional free energy estimates. For asymmetric setups W^- does not satisfy a FR anymore (only W does) and cannot be used to extract free energy differences.

A deep understanding of how to correctly define and measure thermodynamic work in small systems (a long debated question in the past 20 years) is not just a fine detail for experimentalists and theorists working in the single molecule field, but an essential question pertaining to all areas of modern science interested in energy transfer processes at the nanoscale. The new added feature of free energy inference discovered in this paper paves the way to apply FRs to new problems and contexts. This remains among the most interesting open problems in this exciting field.

Methods

Buffers and DNA substrates. All experiments were performed in PBS Buffer 1M NaCl at 25°C; 1 mg/ml BSA was added to passivate the surfaces and avoid nonspecific interactions. The dsDNA tether was obtained ligating a 1kb segment to a biotin-labeled oligo at one end and a dig-labeled oligo at the other end. The DNA hairpin used in the experiments has short (20bp) molecular handles and was synthesized by hybridization and ligating three different oligos. One oligo is biotin-labeled and a second is dig-labeled. Details of the synthesis procedure are given in [33].

Optical Tweezers Assay. Measurements were performed with a highly stable miniaturized laser tweezers in the dual trap mode [32]. This instrument directly measures forces by linear momentum conservation. In all experiments we used silica beads with 4 μm diameter, which give a maximum trapping force around 20 pN. Data is acquired at 1 kHz.

Acknowledgements

We thank A. Alemany and M. Palassini for a critical reading of the manuscript. FR is supported by ICREA Academia 2008 grant. The research leading to these results has received funding from the European Union Seventh Framework Programme (FP7/2007-2013) under grant agreement n° 308850 INFERNOS.

References

- [1] Hummer G, Szabo A (2001) Free energy reconstruction from nonequilibrium single-molecule pulling experiments. *Proceedings of the National Academy of Sciences* 98:3658–3661.
- [2] Hummer G, Szabo A (2010) Free energy profiles from single-molecule pulling experiments. *Proceedings of the National Academy of Sciences* 107:21441–21446.
- [3] Liphardt J, Dumont S, Smith SB, Tinoco I, Bustamante C (2002) Equilibrium information from nonequilibrium measurements in an experimental test of Jarzynski’s equality. *Science* 296:1832–1835.

- [4] D. Collin, et al. (2005) Verification of the Crooks fluctuation theorem and recovery of RNA folding free energies. *Nature* 437:231–234.
- [5] Gupta A, et al. (2011) Experimental validation of free energy-landscape reconstruction from non-equilibrium single-molecule force spectroscopy measurements. *Nature Physics* 7:631–634.
- [6] Alemany A, Mossa A, Junier I, Ritort F (2012) Experimental free energy measurements of kinetic molecular states using fluctuation theorems. *Nature Physics* 8:688–694.
- [7] Dhakal S, et al. (2010) Coexistence of an ILPR i-motif and a partially folded structure with comparable mechanical stability revealed at the single-molecule level. *Journal of the American Chemical Society* 132:8991–8997.
- [8] Dhakal S, et al. (2013) Structural and mechanical properties of individual human telomeric G-quadruplexes in molecularly crowded solutions. *Nucleic Acids Research* 41:3915–3923.
- [9] Cecconi C, Shank E, Bustamante C, Marqusee S (2005) Direct observation of the three-state folding of a single protein molecule. *Science* 309:2057–2060.
- [10] Shank E, Cecconi C, Dill J, Marqusee S, Bustamante C (2010) The folding cooperativity of a protein is controlled by its chain topology. *Nature* 465:637–640.
- [11] Gebhardt J, Bornschlöggl T, Rief M (2010) Full distance-resolved folding energy landscape of one single protein molecule. *Proceedings of the National Academy of Sciences* 107:2013–2018.
- [12] Yu H, et al. (2012) Energy landscape analysis of native folding of the prion protein yields the diffusion constant, transition path time, and rates. *Proceedings of the National Academy of Sciences* 109:14452–14457.
- [13] Harris N, Song Y, Kiang C (2007) Experimental free energy surface reconstruction from single-molecule force spectroscopy using Jarzynski’s equality. *Physical Review Letters* 99:68101–68104.

- [14] Bizzarri A, Cannistraro S (2010) Free energy evaluation of the p53-mdm2 complex from unbinding work measured by dynamic force spectroscopy. *Phys. Chem. Chem. Phys.* 13:2738–2743.
- [15] Jarzynski C (1997) Nonequilibrium equality for free energy differences. *Physical Review Letters* 78:2690–2693.
- [16] Crooks GE (1999) Entropy production fluctuation theorem and the nonequilibrium work relation for free energy differences. *Physical Review E* 60:2721–2726.
- [17] Douarche F, Ciliberto S, Petrosyan A (2005) Estimate of the free energy difference in mechanical systems from work fluctuations: experiments and models. *Journal of Statistical Mechanics: Theory and Experiment* 09:P09011
- [18] Mossa A, de Lorenzo S, Huguet JM, Ritort F (2009) Measurement of work in single-molecule pulling experiments. *The Journal of Chemical Physics* 130:234116–234125.
- [19] Alemany A, Ribezzi-Crivellari M, Ritort F (2011) *in* Nonequilibrium Statistical Physics of Small Systems: Fluctuation Relations and Beyond, eds Klages R, Just W, Jarzynski C (Wiley-VCH, Weinheim) pp 155–179.
- [20] van Mameren J, et al. (2008) Counting rad51 proteins disassembling from nucleoprotein filaments under tension. *Nature* 457:745–748.
- [21] Cisse I, Mangeol P, Bockelmann U (2011) *in* Single Molecule Analysis, eds Peterman EJG, Wuite GJL (Humana Press, New York) pp 45–61.
- [22] Moffitt J, Chemla Y, Izhaky D, Bustamante C (2006) Differential detection of dual traps improves the spatial resolution of optical tweezers. *Proceedings of the National Academy of Sciences* 103:9006–9011.
- [23] Speck T, Mehl J, Seifert U (2008) Role of external flow and frame invariance in stochastic thermodynamics. *Physical Review Letters* 100:178302–178305.
- [24] Mazonka O, Jarzynski C (1999) Exactly solvable model illustrating far-from-equilibrium predictions. *arXiv preprint cond-mat/9912121*.

- [25] Wang G, Sevick EM, Mittag E, Searles DJ, Evans DJ (2002) Experimental demonstration of violations of the second law of thermodynamics for small systems and short time scales. *Physical Review Letters* 89:50601–50604.
- [26] Meiners JC, Quake SR (1999) Direct measurement of hydrodynamic cross correlations between two particles in an external potential. *Physical Review Letters* 82:2211–2214.
- [27] Gore J, Ritort F, Bustamante C (2003) Bias and error in estimates of equilibrium free energy differences from nonequilibrium measurements. *Proceedings of the National Academy of Sciences* 100:12564–12569.
- [28] Palassini M, Ritort F (2011) Improving free energy estimates from unidirectional work measurements: theory and experiment. *Physical Review Letters* 107:60601.
- [29] Ritort F, Bustamante C, Tinoco I (2002) A two-state kinetic model for the unfolding of single molecules by mechanical force. *Proceedings of the National Academy of Sciences* 99:13544–13548.
- [30] Jarzynski C (2006) Rare events and the convergence of exponentially averaged work values. *Phys. Rev. E* 73:046105–046114.
- [31] Ribezzi-Crivellari M, Ritort F (2012) Force spectroscopy with dual-trap optical tweezers: Molecular stiffness measurements and coupled fluctuations analysis. *Biophysical journal* 103:1919–1928.
- [32] Ribezzi-Crivellari M, Huguet JM, Ritort F (2013) Counter-propagating dual-trap optical tweezers based on linear momentum conservation. *Review of Scientific Instruments* 84:043104–043104.
- [33] Forns N, De Lorenzo S, Manosas M, Hayashi K, Huguet JM, Ritort F (2011) Improving signal/noise resolution in single-molecule experiments using molecular constructs with short handles. *Biophysical journal* 100:1765–1774.

Caption of Figure 1

Pulling experiments with dual-trap optical tweezers. A) Force-distance curves in a pulling experiment on a 20 bp hairpin with our dual-trap setup.

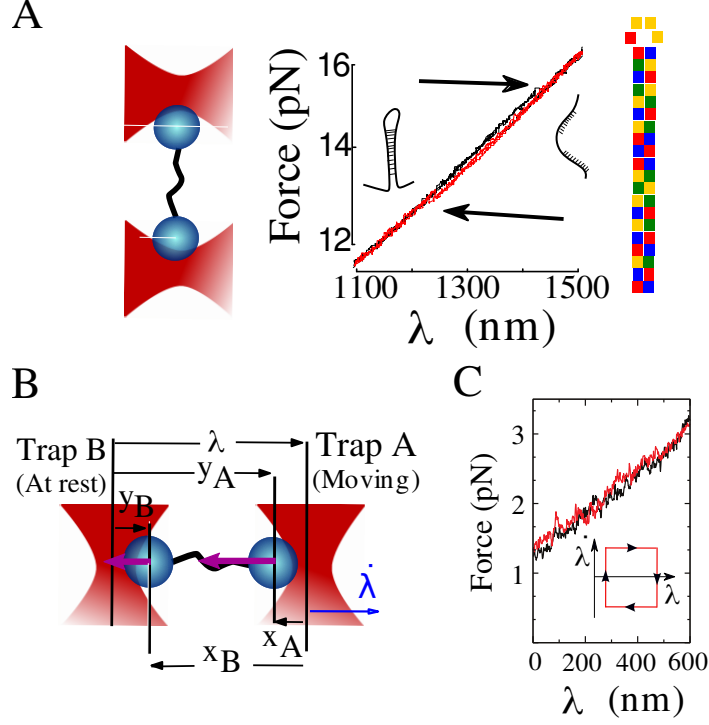


Figure 1:

A molecular tether is attached between two trapped beads. By increasing the distance, λ , between the traps the tether is stretched or released until some thermally activated reaction is triggered, e.g. the unfolding or folding of a DNA hairpin, and detected as a force jump (black arrows). The small force jump (0.2 pN) is due to the low-trap stiffness of our dual-trap setup ($\simeq 0.02$ pN/nm). Inset: scheme of the hairpin with color-coded sequence (A/T: yellow/green, G/C: red/blue). B) Pulling experiments in a dual-trap setup where trap A is moved at speed $\dot{\lambda}$ and trap B is at rest with respect to water. λ is the control parameter, y_A and y_B are the configurational variables with respect to the moving trap A while x_A and x_B are the configurational variables with respect to the trap at rest (trap B). C) pulling curves (red stretching, black releasing) for a 3kb ds-DNA tether in a dual-trap setup. Inset: the cyclic pulling protocol used in the experiments.

Caption of Figure 2

Work Distributions. Work statistics obtained on cyclic protocols with a 200 nm excursion with different pulling speeds (columns). Four different work observables are considered. In each case the solid points are direct work measurements (l.h.s. of Eq. (27)). In order to improve statistics these distributions are calculated as the convolution of the distribution of the work performed while stretching with that performed while releasing. For that we took all forward and reverse work values W_F, W_R and combined them $W = W_F + W_R$ in order to get a joint work distribution for the cycle. Open symbols are the reconstructed histogram (r.h.s. of Eq. (27)). Different columns refer to different pulling speeds, $\dot{\lambda}$, as shown on top. A) Comparison of the measured and reconstructed distributions according to the two definitions of Eq. (25) (D, D'). The distribution for D satisfies the CFR Eq.(27), i.e. the measured and reconstructed distributions superimpose. The distribution for D' does not satisfy it. Horizontal error bars represent the systematic error in work measurements, while vertical error bars denote statistical errors. B) The CFR, Eq. (27) is satisfied within the experimental error for D, D^+ and D^- but not for D' . C) Comparison between the measured and reconstructed distributions for D^- and D^+ (Eq.(28) and Eq. (29)) both of which satisfy the CFR. Horizontal error bars represent the systematic error in work measurements, while vertical error bars denote statistical errors.

Caption for Figure 3

Bias in unidirectional free energy estimators. A) Error (\mathcal{E}) on free energy estimates Eq. (12) committed by using JE for W' . Circles, diamonds and squares refer to excursions of 200 nm, 400 nm and 600 nm. Three different pulling speeds were considered in each case. Note that in this case work is evaluated over closed cycles ($\Delta G = 0$) and the error is defined as: $\mathcal{E} = -\beta^{-1} \log \langle e^{-\beta W'} \rangle$. B) $\langle W^+ \rangle$ displays a bilinear dependence on pulling speed $\dot{\lambda}$ (Main Figure) and $\Delta \lambda$ (Inset) as expected from Eq. (17). Continuous lines are linear fits to the experimental results which contains a single fitting parameter. The shaded area in the inset corresponds to the region within one standard deviation from the expected value of $\langle W^+ \rangle$ based on equilibrium measurements of γ_+ (see Section 4,5 in the SI). C) Experimental bias measurements from the cycles shown in Fig. 1C. The plots show the

bias (Eqs. (22),(23)) as a function of the number of work measurements, N . The three plots correspond to different pulling speeds ($7.2 \mu\text{m/s}$, $4.3 \mu\text{m/s}$, $1.35 \mu\text{m/s}$). Interestingly $B_N^- \ll B_N$ which guarantees faster convergence of free energy estimates. Moreover B_N is also larger than the sum $B^- + B^+$ (dashed line) i.e. the bias is superadditive (cf. Eq. (24)). The error bars represent the statistical error on free energy determination, not including systematic calibration errors in force and distance. Continuous lines show the theoretical predictions from Ref. [28] for Gaussian work distributions. Note that these are not fits but predictions which only use the mean dissipation as input parameter.

Caption for Figure 4

Work measurements on a DNA hairpin. A) Scheme of the experimental setup (beads and hairpin not to scale). The hairpin is presented with color-coded sequence (A/T: yellow/green, G/C: red/blue). B) Work measurements upon unfolding and refolding according to three different work definitions: W (upper panel), W' (central panel) and W^- (lower panel). In this experiment pulling speed was $0.96 \pm 0.02 \mu\text{m/s}$. Open symbols show an estimate of the refolding work distributions reconstructed from the unfolding distribution via the CFR (Eq. (26)). W and W^- fulfill the fluctuation theorem while W' does not. Horizontal error bars represent the systematic error on work measurements, while vertical error bars denote statistical errors. The contribution of trap, handles and single stranded DNA have been removed as detailed in [6]. C) Unidirectional estimates for the free energy from the unfolding work distribution. The optimal estimator based on W^- (red) converges to the correct value $\Delta G_0 = 51 K_B T$ as measured from bi-directional estimates. The estimator based on W (green) shows a larger bias and overestimates the free energy by $\simeq 1 K_B T$. The estimator based on W' (blue) converges to a wrong free energy difference ($\Delta G - \mathcal{E}$) which is $\simeq 3 K_B T$ below the correct value, against the second law. Note that the error committed by using W is due to finite-size effects and decreases when more unfolding curves are measured. In contrast the error committed by using W' remains finite for all sample sizes. The error bars represent the statistical error on free energy determination and do not include the systematic error due to force and distance calibrations.

Caption for Figure 5

Inference of $P(W)$ from partial work measurements in the symmetric case. A) The distribution $P'(W')$ in the case of the dsDNA tether, for the work measured in the wrong trap, W' . The distribution does not fulfill the CFR. To recover the correct work distribution $P(W)$, W' is shifted by a constant amount Δ . The shifted distribution is tested for the CFR by defining the function: $H(W') = \log(P'(W' - \Delta)/P'(-W' - \Delta))$. The prediction by the CFR is $H(W') = \beta(W' - \Delta G)$ which can be tested by determining the H function. B) Evolution of $H(W')$ as a function of W' for different values of Δ . The value Δ^* for which the slope of $H(W')$ is equal to one (work being measured in $K_B T$ units) determines the correct work distribution $P(W)$ ($\Delta \simeq 15$, inset). C) In the case of bidirectional measurements both the forward and the reverse work distributions $P'_F(W')$, $P'_R(-W')$ are shifted by an amount Δ in opposite directions. D) Evolution of the function $H = \log(P'_F(W' - \Delta)/P'_R(-W' - \Delta))$ as a function of Δ . Again the CFR predicts H should be linear in W' with slope one. E) Inference of the correct work distributions and ΔG measurement. For each value of Δ a linear fit $A(\Delta)W + B(\Delta)$ to H is performed. The value Δ^* for which $A(\Delta^*) = 1$ ($\Delta^* \simeq 7$ in the figure), is the shift needed in order to recover the full work distribution $P(W)$ from partial work measurements in the wrong trap. Moreover the CFR implies $B(\Delta^*) = -\Delta G$ ($\Delta G \simeq 60 K_B T$).

Caption for Figure 6

Inference of $P(W)$ from partial work measurements in the asymmetric case. (A) Equilibrium force distributions at 2pN for the 3kb ds-DNA tether measured in an asymmetric dual-trap setup ($k_A = 0.012$ pN/nm, $k_B = 0.003$ pN/nm, $k_m = 0.0027$ pN/nm). (B) Convolution of $P'(W')$ with different Gaussian distributions corresponding to different pairs Δ, Σ . We show $P'(W)$ (blue filled circles), $P'(-W) \exp(\beta W)$ (blue empty circles), $P(W)$ (green filled circles). Among all different $P_{\Delta, \Sigma}$ only one matches the correct work distribution $P(W)$, i.e. only one reconstructed distribution is physically correct (rightmost graph, with $\Delta = 7.5 K_B T$, $\Sigma^2 = 8 (K_B T)^2$). In this situation the inference cannot rest on the CFR alone, and additional information is required to infer $P(W)$. (C) Asymmetry factor (AF) as a function of $x = k_A/k_B$ for different values of $y = k_m/k_B$. The blue (red)

circles indicate the symmetric ($AF = 0$) and asymmetric ($AF \simeq 1$) cases respectively. (D) The AF defined by $\Sigma^2 = AF \times \Delta$ (red line) and the CFR invariance $\Delta = \Delta^* + \phi, \Sigma^2 = \Sigma^{*2} + 2\phi K_B T$ for any ϕ (blue line), do select a narrow range of possible pairs (Δ, Σ) at the intersection between the blue and red lines. The intersection region is compatible with the parameters ($\Delta = 8 K_B T, \Sigma^2 = 7.2 (K_B T)^2$) describing the true correct work distribution $P(W)$ (black point).

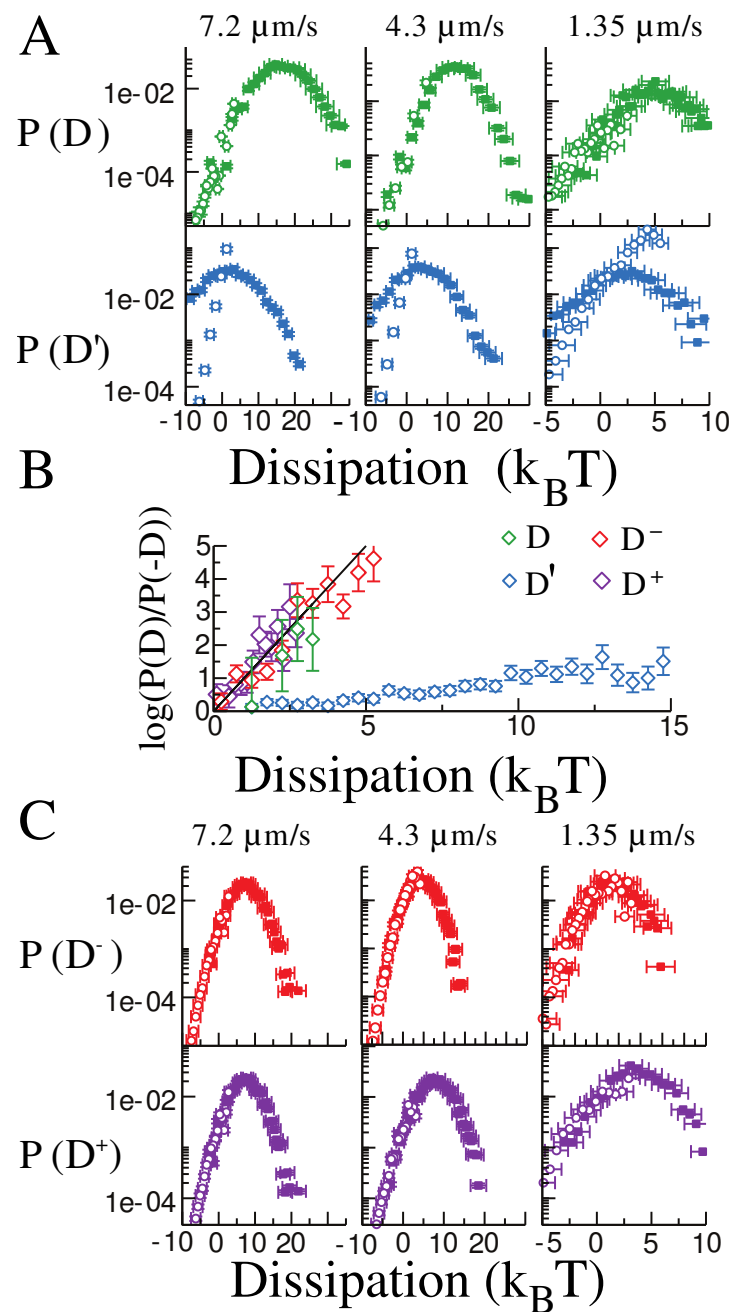


Figure 2:

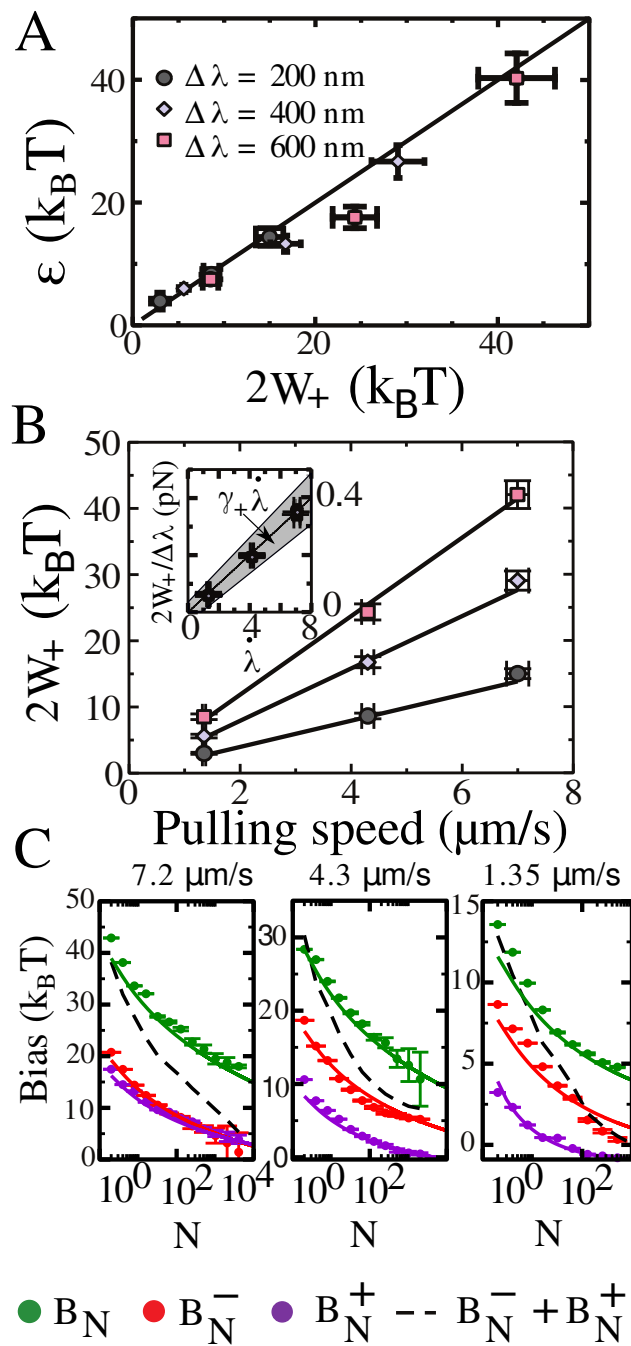


Figure 3:

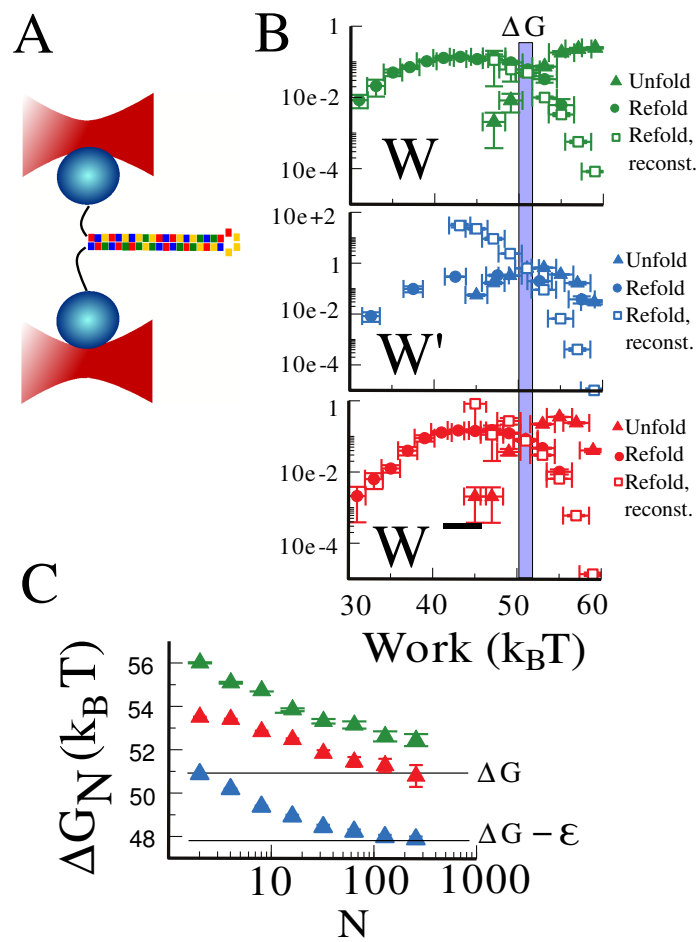


Figure 4:

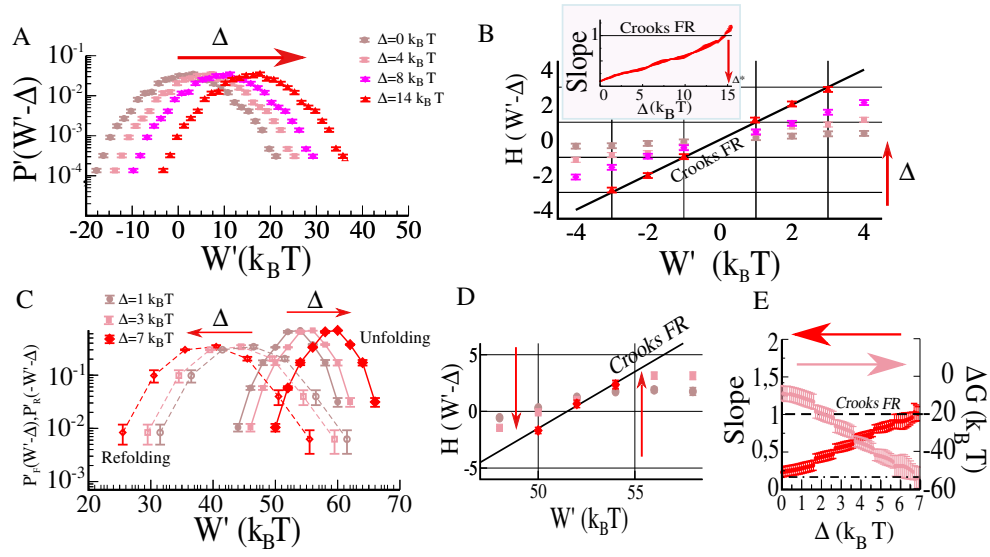


Figure 5:

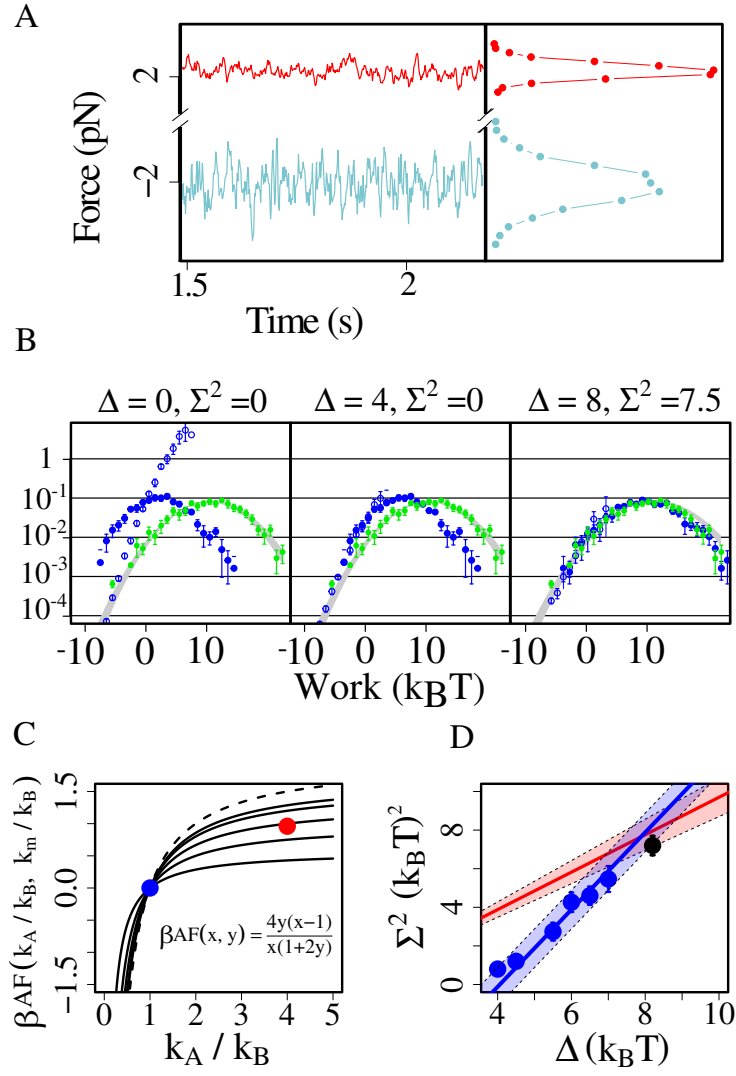


Figure 6:

Supporting information to: "Free energy inference from partial work measurements in small systems"

M. Ribezzi-Crivellari¹ and F. Ritort^{1,2}

¹Departament de Física Fonamental, Universitat de Barcelona

²Ciber-BBN de Bioingeniería, Biomateriales y Nanomedicina

Contents

1	A model for the experimental setup	2
2	The differential x_- and center-of-mass x_+ coordinates are statistically independent	3
3	The differential work W_- and W_+ are statistically independent	4
4	Direct measurement of the hydrodynamic parameters	5
5	A closer look to hydrodynamic interactions	6
6	Free energy inference in asymmetric setups	7
6.1	Pulling experiments in linear systems	8
6.2	W and W' as Gaussian random variables	9
6.3	The AF can be measured from equilibrium force traces	11
6.4	Derivation of the expression for the AF	12
6.5	Derivation of the equations	12
6.6	Solution of the equations	14
7	Experiments at lower pulling speed	17

In this document we analyze in further detail several aspects of the manuscript regarding theory and experiments. Concerning the theory we study in detail a dynamical model describing the experiments reported in the main text. This model is then used to shed light on several aspects of the discussion in the main text. In section S1 we introduce the model in the symmetric case. In section S2 we prove that x_+ and x_- are independent quantities in our model, which is a central result in our discussion. In section S3 we do the same for W_+ and W_- . These conclusions are supported by a statistical analysis of the experimental data. In sections S4 and S5 we comment on the definition and meaning of the hydrodynamic parameters of our model. One of these parameters is γ_+ , which was used in estimating the missing contribution to the total dissipation when using the wrong work definition W' . We will also recall how to measure these parameters from equilibrium experiments and present measurements on different DNA tethers. In section S6 we will discuss free energy inference in asymmetric setups and in section S7 we present measurements at lower pulling speeds. These measurements show that correct work measurements is important even at low irreversibility conditions.

S1 A MODEL FOR THE EXPERIMENTAL SETUP

We consider a model for the experimental dual-trap setup shown in Fig. S1. In this setup two focused laser beams form two optical traps, which allow us to manipulate a dumbbell formed by two trapped beads coupled through a molecular tether. The model is one dimensional: the dynamics takes place along the direction of the tether, y -axis in Fig. S1. Should the tether not be oriented in the plane perpendicular to the direction of the laser beams, the analysis is more involved as detailed in Ref. [1]. In this section we will assume the two traps are identical and harmonic, so that the total potential energy reads:

$$U_{\text{TOT}}(y_A, y_B) = \frac{k}{2} y_B^2 + \frac{k}{2} (y_A - \lambda)^2 + U_m(y_A - y_B). \quad (1)$$

A more general discussion, taking into account asymmetric setups, will be deferred to section S6. Note that we choose the center of trap B (left trap) as the origin of our reference frame and that λ is the position of trap A relative to trap B. A dynamical model for our system can be obtained using Langevin equations subject to a total potential as defined in Eq. (1):

$$\dot{\mathbf{y}} = -\bar{\mu} \nabla U_{\text{TOT}}(y_A, y_B, \lambda_t) + \boldsymbol{\eta}, \quad (2)$$

where $\mathbf{y} = (y_A, y_B)$, $\nabla = (\partial_{y_A}, \partial_{y_B})$, $\boldsymbol{\eta} = (\eta_A, \eta_B)$ is a vector formed by the noise terms affecting the two beads and $\bar{\mu}$ is the mobility tensor. We assume the noise to be δ correlated in time, and the Fluctuation-Dissipation Theorem to be fulfilled:

$$\langle \boldsymbol{\eta}_i(s) \boldsymbol{\eta}_j(t) \rangle = K_B T \mu_{i,j} \delta(t - s), \quad (3)$$

i.e. that the covariance of the noise is proportional to the mobility μ . In the above expression K_B is the Boltzmann constant and T the absolute temperature. In the vector Equation (2) the mobility is a tensor or matrix. Its diagonal terms describe the friction affecting the motion of the beads, while the off-diagonal terms describe hydrodynamic interactions between the beads:

$$\bar{\mu} = \begin{pmatrix} \gamma_A^{-1}(y_A, y_B) & \Gamma_{AB}^{-1}(y_A, y_B) \\ \Gamma_{BA}^{-1}(y_A, y_B) & \gamma_B^{-1}(y_A, y_B) \end{pmatrix}.$$

The validity of Eq. (3) for hydrodynamic fluctuations in a pulling experiment is a standard assumption, and it is a necessary hypothesis in the derivation of FRs such as Jarzynski equality or the Crooks fluctuation relation. The analysis of this equation is greatly simplified by the following two features, which can be easily matched in our experimental setup:

- The setup is fully symmetric, meaning not only $k_A = k_B$ but also $r_A = r_B$ where r_A, r_B are the bead radii.

- The hydrodynamic coefficients γ, Γ between the beads do not significantly change in the force range of a pulling experiment. In section S4 we show that this condition is met for tethered molecules ranging from 20 nm to 1 μm in contour length to a 10% accuracy.

This guarantees that the mobility matrix is symmetric and constant:

$$\mu = \begin{pmatrix} \gamma^{-1} & \Gamma^{-1} \\ \Gamma^{-1} & \gamma^{-1} \end{pmatrix}.$$

Under these conditions, the transformation $x_+ = \frac{y_A + y_B}{2}, x_- = y_B - y_A$, decouples the potential into two separate terms,

$$U_{\text{TOT}}(x_-, x_+; \lambda) = U^-(x_-; \lambda) + U^+(x_+; \lambda).$$

Moreover the symmetry requirements cited above have the following two important consequences:

- It diagonalizes the mobility tensor μ in the form:

$$\mu = \begin{pmatrix} \gamma_+^{-1} & 0 \\ 0 & \gamma_-^{-1} \end{pmatrix}.$$

- It diagonalizes the noise covariance, i.e. it gives rise to two statistically independent noise contributions, η_+ and η_- which separately affect the new coordinates x_+ and x_- :

$$\langle \eta_{\pm}(s) \eta_{\pm}(t) \rangle = K_B T \gamma_{\pm} \delta(t - s), \quad \langle \eta_+(s) \eta_-(t) \rangle = 0. \quad (4)$$

In the main text we have shown how the partition functions for x_- and x_+ decouple. From previous equations one can easily see that the full right-left symmetry of the setup guarantees that also the equations of motion for x^+ and x^- decouple completely:

$$\gamma_+ \dot{x}_t^+ = -\partial_{x^+} U^+(x_t^+, \lambda_t) + \eta_t^+ \quad (5)$$

$$\gamma_- \dot{x}_t^- = -\partial_{x^-} U^-(x_t^-, \lambda_t) + \eta_t^-. \quad (6)$$

S2 THE DIFFERENTIAL X_- AND CENTER-OF-MASS X_+ COORDINATES ARE STATISTICALLY INDEPENDENT

The factorization of the partition function (Eq.8 in the main text) plays an important role in the derivation of our results. For symmetric systems such factorization is directly related to the statistical independence of the center of mass and differential coordinates. Here we experimentally check this factorization by showing how we can generally describe the state of our system using a decomposition of the measured forces into two statistically independent coordinates. For linear systems such decomposition is always possible whereas for general non-linear systems such decomposition is only possible in the symmetric case. Imagine that the equilibrium distribution of our system is dictated by a Hamiltonian depending on two coordinates: $U(y_A, y_B)$, which takes the form $U_+(x_+) + U_-(x_-)$ for a general transformation, $x_- = x_-(y_A, y_B)$ and $x_+ = x_+(y_A, y_B)$. In this situation, x_+ and x_- are statistically independent:

$$P(x_+ | x_-) = P(x_+) \propto \exp(-\beta U_+(x_+)), \quad (7)$$

and in particular have zero covariance:

$$\langle x_+ x_- \rangle = \langle x_- \rangle \langle x_+ \rangle. \quad (8)$$

A further consequence of this decomposition of the Hamiltonian is the factorization of the partition function discussed in the main text. For simplicity we will be considering forces instead of distances, as our instrument directly measures forces. The independence of the coordinates x_+ and x_- directly translates into the independence of the corresponding forces:

$$f_+ = -\partial U_+(x_+) \quad f_- = -\partial U_-(x_-), \quad (9)$$

indeed:

$$\langle f_+ f_- \rangle = \int dx_+ dx_- f_+ f_- e^{-\beta U} = \int dx_+ f_+ e^{-\beta U_+} \int dx_- f_- e^{-\beta U_-} = \langle f_+ \rangle \langle f_- \rangle. \quad (10)$$

We shall use the covariance as a measure of linear dependence and a Pearson's χ^2 test as a measure of dependence in general. The χ^2 test is described below in section S3 of this document. The transformations we use to uncouple the two degrees of freedom are rotations of the form:

$$f_+^\phi = \cos(\phi) f_A + \sin(\phi) f_B \quad (11)$$

$$f_-^\phi = -\sin(\phi) f_A + \cos(\phi) f_B \quad (12)$$

We present measurements of equilibrium force fluctuations obtained using different tethers. In Figure S2 we describe measurements performed on 1kb dsDNA tethers stretched at 2 pN. Experiments were performed using PBS buffer (pH 7.5), 1M NaCl at 25 Celsius degrees just as in the pulling experiments described in the main text. The force of 2pN was chosen to fall in the range explored in the pulling experiments. The first set of measurements was performed using symmetric traps $k_A \simeq k_B \simeq 0.02$ pN/nm. The second set of experiments was performed with asymmetric traps, $k_A = 0.012$ pN/nm, $k_B = 0.003$ pN/nm. In both cases it is possible to find a coordinate system such that the two coordinates are independent and in both cases this coordinate system is obtained by a rotation of the vector (f_A, f_B) (Fig. S2A,C). The difference is that in the symmetric case the new variables correspond to the center-of-mass and differential coordinate as discussed in the main text (Fig S2B), while they have a different definition (i.e. they are not generated by a $\pi/4$ rotation) in the asymmetric case (Fig. S2D). In Figure S3 we report similar measurements performed on a DNA hairpin (the sequence is the same reported in the main text) in a symmetric setup. Equilibrium traces were acquired at different forces. From top to bottom we can see the hairpin is 1) completely folded, 2) preferentially folded, 3) preferentially unfolded, 4) completely unfolded. Force fluctuations are clearly non-Gaussian, a characteristic of non-linear two-state systems. Again, for the symmetric setup, our data show that the center of mass (x_+) and differential coordinate (x_-) are independent. We note that in the more general non-linear case and for asymmetric setups no independent coordinates can be defined.

S3 THE DIFFERENTIAL WORK W_- AND W_+ ARE STATISTICALLY INDEPENDENT

An immediate consequence of the decoupling of the equations of motion is the independence of W_+ and W_- :

$$W_\pm = \int \partial_\lambda U_\pm(x_\pm, \lambda) \dot{\lambda} dt.$$

Now, since W^+ does only depend on x^+ and W^- does only depend on x^- we can conclude that the two quantities are independent. Of course this results holds under specific assumptions and is, in the end, just a property of the model. From the experimental point of view one can test the independence of W^+ and W^- by statistical analysis, studying their linear (Pearson) correlations or using a Pearson's χ^2 test for dependence. The first method is sensitive to linear correlation between two observables, while the second, more stringent test, is sensitive to generic correlations. The χ^2 test goes as follows: to test the independence of two random variables (A, B) from a finite number of measurements we first define the empirical marginals, i.e. separate histograms of the two variables:

$$e_j^a = \sum_i^N \delta(A_i \in [a_j, a_{j+1}))/N \quad (13)$$

$$e_j^b = \sum_i^N \delta(B_i \in [b_j, b_{j+1}))/N, \quad (14)$$

here $\delta(x \in \mathcal{C})$ is 1 if x belongs to the set \mathcal{C} and is 0 otherwise. We then compare the actual two-dimensional histogram, e_{ij} to the product of the marginals:

$$\chi^2 = \sum_{k,l} \frac{(e_{kl} - e_k^a e_l^b)^2}{e_k^a e_l^b}, \quad (15)$$

with $e_{jk} = \sum_i \delta(A_i \in [a_j, a_{j+i})) \delta(B_i \in [b_k, b_{k+i})) / N$. The value obtained through Eq. (15) is then compared to the χ^2 distribution. The two variables are considered independent if the χ^2 value satisfies 5% significance test. The results of the two statistical tests is reported in Table S1 and S2. These tables compare the result of the tests performed on the pair W, W' or on the pair W_+, W_- , for the forward, the reverse and the cyclic protocols. In each case three different pulling speeds are considered. The two different tables refer to two different dumbbells. In most cases the pair W, W' shows higher covariance than the pair W_+, W_- . Moreover the χ^2 test detects dependence between W, W' but not between W_+, W_- (in the χ^2 column 1 denotes a positive test for dependence and 0 a negative test).

S4 DIRECT MEASUREMENT OF THE HYDRODYNAMIC PARAMETERS

In the main text we have already shown how, in a symmetric setup, by changing to the coordinate system defined by the center of mass and differential coordinates x_+, x_- , the potential decouples into two terms:

$$U_{\text{TOT}}(x_+, x_-) = k(x_+ - \frac{\lambda}{2})^2 + \frac{k}{4}(x_- - \lambda)^2 + U_m(x_-). \quad (16)$$

When considering equilibrium fluctuations at constant trap-to-trap distance λ , a linear approximation of U_m in Eq. (16) may be used. The energy has a minimum at $x_+ = \lambda$, $x_- = x_-^0$. The value of x_-^0 is defined by:

$$\partial_{x_-} U_{\text{TOT}} \Big|_{x_-^0} = 0. \quad (17)$$

Here x_-^0 is the (mechanical) equilibrium distance between the centers of the beads. The position of the minimum and the derivative of the potential at the minimum depend on the trap-to-trap distance, so that x_-^0 is a function of λ . In this approximation the equations of motion in Eq. (5) become:

$$\gamma_+ \dot{x}_+ = -2k \left(x_+ - \frac{\lambda}{2} \right) + \eta_+, \quad (18)$$

$$\gamma_- \dot{x}_- = - \left(\frac{k}{2} + k_m \right) (x_- - x_-^0) + \eta_-. \quad (19)$$

In particular γ_+ is the friction affecting the center of mass of the dumbbell, while γ_- affects the dynamics of the differential coordinate. After Bachelors [3] we set:

$$\gamma_+^{-1} = (\gamma^{-1} + \Gamma^{-1}) / 2, \quad \gamma_-^{-1} = 2 (\gamma^{-1} - \Gamma^{-1}). \quad (20)$$

In brief, γ is the hydrodynamic friction coefficient for a single bead, while Γ is the intensity of hydrodynamic interactions between the two beads. It is important to bear in mind that in principle γ and Γ depend on the differential coordinate x_- . This dependence is negligible in pulling experiments which induce a small change in x_- , but it becomes clear and measurable if x_- is changed to a larger extent, e.g. using molecules of different contour length. The equilibrium probabilities generated by (18),(19) are given by Boltzmann's distribution:

$$Q_{eq}(x_+) = \frac{1}{Z_+} \exp \left(-\beta k (x_+ - \frac{\lambda}{2})^2 \right), \quad (21)$$

$$P_{eq}(x_-) = \frac{1}{Z_-} \exp \left(-\beta \frac{k + 2k_m}{4} (x_- - x_-^0)^2 \right), \quad (22)$$

with Z_+, Z_- normalization factors. The variance of equilibrium fluctuations in x_+ and x_- is connected to the elastic properties of traps and tether by:

$$\sigma_+^2 = \frac{K_B T}{2k}, \quad \sigma_-^2 = \frac{2K_B T}{k + 2k_m}. \quad (23)$$

Information about the hydrodynamic interactions can be obtained from the time-dependent correlation functions of x_+ and x_- :

$$C_+(t) = \langle (x_+(t) - \frac{\lambda}{2})(x_+(0) - \frac{\lambda}{2}) \rangle \quad (24)$$

$$C_-(t) = \langle (x_-(t) - x_-^0)(x_-(0) - x_-^0) \rangle, \quad (25)$$

which characterizes the decay of fluctuations and allows to distinguish the presence of different contributions to the total variance. The computation of the correlation functions yields:

$$\beta C_+(t) = \frac{e^{-k\gamma_+^{-1}t}}{2k}, \quad (26)$$

$$\beta C_-(t) = \frac{2e^{-(k+2k_m)\gamma_-^{-1}t}}{k + 2k_m}, \quad (27)$$

where $\beta = (K_B T)^{-1}$. From Eqs. (24),(25) the correlation function at time 0 equals the variances given in Eq. (23):

$$C_+(0) = \sigma_+^2, \quad C_-(0) = \sigma_-^2. \quad (28)$$

The hydrodynamic parameters can be retrieved from the correlation functions, as the stiffnesses, k, k_m , are known from Eq. (23) :

$$\frac{1}{\gamma} + \frac{1}{\Gamma} = -\frac{1}{2k} \frac{d}{dt} \log(C_+) \Big|_{t=0} \quad (29)$$

$$\frac{1}{\gamma} - \frac{1}{\Gamma} = -\frac{2}{k + 2k_m} \frac{d}{dt} \log(C_-) \Big|_{t=0}. \quad (30)$$

where we used Equations (20),(26) and (27). As discussed in the main text, γ_+ is needed to correct the error committed by using the force measured in the trap at rest in the Jarzynski Equality (Eq. 17 and 18 in the main text).

S5 A CLOSER LOOK TO HYDRODYNAMIC INTERACTIONS

In the previous section we have shown how the analysis of thermal fluctuations in a dual trap setup allows the measurement of the two scalar parameters entering in the hydrodynamics: γ^{-1} and Γ^{-1} . The sum of the two parameters can be obtained through Eq. (29) from the analysis of the time correlation function for x_+ , Eq. (26) . The difference is instead obtained by a similar analysis on the decay rate of $C_-(t)$. Up to now we have neglected the dependence of the hydrodynamic parameters on the relative distance between the two beads. This is justified provided this relative distance does not change too much in the pulling experiments. Conversely changing the contour length of the molecule by an order of magnitude leads to a larger and detectable change in the hydrodynamic parameters. This offers the possibility of testing our measurements against the theoretical prediction obtained using Stokes equation and expressed as a power series in the reduced distance $\rho = \langle x_- \rangle / r_b$ with r_b the radius of the beads and $\langle x_- \rangle$ the mean of the differential coordinate. (Note that $\langle x_- \rangle > 2r_b$ and thus $\rho > 2$). The two quantities can be computed to arbitrary precision, taking the first two terms of the series expansion reported in [4]:

$$\gamma^{-1} \simeq \frac{1}{6\pi\eta r_b} \left(1 - \frac{15}{4\rho^4} + O(\rho^{-6}) \right) \quad (31)$$

$$\Gamma^{-1} \simeq \frac{1}{6\pi\eta r_b} \left(\frac{3}{2\rho} - \frac{1}{\rho^3} + O(\rho^{-7}) \right). \quad (32)$$

We measured fluctuations using ds-DNA tethers of 4 different contour lengths: 8 μm (24 kbp), 1 μm (3 kbp), 300 nm (1.2 kbp) and 20 nm (58 bp). For each tether fluctuations were measured at different forces. The different length of the tethers used in the experiments is such that ρ assumes values from above 6 down to 2.03, near the minimum value 2 taken when the beads are in contact: hydrodynamic interactions are monitored from the far-field regime ($\rho \gg 2$) to the lubrication limit ($\rho \simeq 2$). The experimental data for γ and Γ can be confronted with predictions Eq. (31),(32) without free parameters as the buffer viscosity and the bead radius are known.

This comparison is shown in Figure S4, the upper plot compares the measured values for γ^{-1} and Γ^{-1} with Eq. (31),(32) (solid lines). For every tether we assumed a single value of ρ and averaged values obtained at different forces. On the force range relevant for pulling experiments, changes in γ^{-1} and Γ^{-1} were below 10%. Theory and data do agree, within the error bars for the longer tethers. The data for the shortest tether show a deviation from expression (31) and probably more terms of the expansion would be needed. Nevertheless in this case the parameters are very close to the contact value, $\rho = 2$, $\gamma^{-1}(2)/\gamma^{-1}(\infty) = \Gamma^{-1}(2)/\gamma^{-1}(\infty) = 0.775$. The precision of these measurements is limited, in our case, by the error with which the radius of the bead is known. One can reduce the dependence of the measured value on the size of the bead by using the ratio between the two parameters, which does not depend on r_b if not through the definition of ρ . The results are shown in the lower plot where the measured data are compared to those obtained from untethered beads. This allows us to conclude that, at least in our conditions and within our experimental resolution, the friction and/or hydrodynamic effect due to the presence of a polymer between the beads is not distinguishable. In particular, knowing the value of γ_+ allows an estimation of the systematic error on unidirectional free energy estimates from single molecule pulling experiments based on wrong work definitions, as detailed in the main text.

S6 FREE ENERGY INFERENCE IN ASYMMETRIC SETUPS

In the case of asymmetric setups $P(W)$ and $P(W')$ do not have such a simple relationship as in the symmetric case. In this case a successful inference cannot be based on the FR alone: some additional, system-specific, information must be provided. We shall focus on asymmetric systems in the Gaussian approximation and use pulling experiments on dsDNA in an asymmetric setup to test our predictions. Is it still possible to infer the full dissipation from partial work measurements? The answer is positive if we are given some equilibrium information on the system. In this case it is enough to know the trap and molecular stiffnesses k_B, k_A, k_m i.e. equilibrium properties of the system. But why does direct inference fail in the asymmetric case? When discussing symmetric systems we have shown that $P(W)$ and $P(W')$ are related by a simple shift:

$$P(W) = P'(W - \Delta). \quad (33)$$

Only the mean of the probability distribution had to be changed, as the variance of the two distributions is the same. In that case imposing the validity of the CFR for $P(W)$ yields the unique value of Δ to be used in the reconstruction. This is not true anymore in asymmetric systems. Here both the mean and the variance of the work distribution must be changed, which can be achieved by convolution:

$$P(W)_{\Delta, \Sigma} = P' \star \mathcal{N}(\Delta, \Sigma), \quad (34)$$

where \star denotes the convolution operator and $\mathcal{N}(\Delta, \Sigma)$ is a normal distribution with mean Δ and standard deviation Σ . Starting from any distribution $P'(W')$ there are infinitely many choices of Δ and Σ which yield a $P(W)_{\Delta, \Sigma}$ satisfying the fluctuations theorem. Indeed, let us suppose the pair Δ^*, Σ^* is such that:

$$P_{\Delta^*, \Sigma^*}(W) = P' \star \mathcal{N}(\Delta^*, \Sigma^*) \quad (35)$$

satisfies the CFR. Then it is easy to check that $P_{\Delta^* + \phi, \sqrt{(\Sigma^*)^2 + 2\phi/\beta}}$ will satisfy the FT for any ϕ ($\beta = 1/K_B T$ as always). In Figure S5 we show the effect of the convolution of $P'(W')$ with different Gaussian distributions. In the rightmost column of that plot we highlight three different pairs for which the convolved distribution satisfies the CFR. In this situation the inference cannot rest on the CFR alone, and additional information about the system is needed. In the general scheme of a Gaussian approximation,

inference of $P(W)$ is still possible. In the coming subsections we will show that $P(W)$ and $P'(W')$ are related by an Asymmetry Factor (AF) given by:

$$AF(k_A, k_m, k_B) = \frac{\sigma_W^2 - \sigma_{W'}^2}{\langle W \rangle - \langle W' \rangle} = \frac{1}{\beta} \frac{4k_m(k_A - k_B)}{k_A(k_B + 2k_m)}, \quad (36)$$

where $\beta = 1/K_B T$. The AF is an equilibrium quantity: it only depends on the stiffnesses of traps and tether. Knowing the AF allows us to select the unique pair (Δ, Σ) such that $AF = \Sigma^2/\Delta$ and that $P_{\Delta, \Sigma}(W)$ satisfies the fluctuation symmetry. These (Δ, Σ) allow the reconstruction of $P(W)$ and thus to measure free energy differences or even dynamical quantities like γ_+ . The behavior of the AF factor as a function of $x = k_B/k_A$ and $y = k_m/k_A$ is shown in the left panel of Figure S6.

S6.1 PULLING EXPERIMENTS IN LINEAR SYSTEMS

Free energy inference in asymmetric setups is not as straightforward as it is in symmetric setups. In order to recover the full dissipation from partial work measurements we must complement these non-equilibrium measurements with some equilibrium information about the system. In this section we will consider a Gaussian approximation for asymmetric setups that, as shown in Figure 6 in the main text, agrees pretty well with the experimental results. The Gaussian case will be modelled by linear asymmetric systems, a class of statistical models for which inference is possible without symmetry restrictions. This amounts to choosing $U_m(x) = \frac{1}{2}k_m x^2$ in Eq. 1 so that the total potential reads:

$$U(y_A, y_B, \lambda) = \frac{k_m}{2}(y_B - y_A)^2 + \frac{k_B}{2}y_B^2 + \frac{k_A}{2}(\lambda - y_A)^2. \quad (37)$$

In order to simplify the following discussion we will now switch to a vector notation. From now on we shall denote with $\mathbf{X}^T(t)$ the vector containing the positions of the traps (remind that B is the reference trap at rest with respect to water while trap A moves):

$$\mathbf{X}^T(t) = (\lambda_t, 0), \quad (38)$$

and with \mathbf{y} the vector of bead positions: $\mathbf{y} = (y_A, y_B)$. In this vector notation the potential can be written in its normal form as:

$$U(\mathbf{y}, \mathbf{X}^T(t)) = \frac{1}{2}(\mathbf{y} - \mathbf{y}^0) \cdot \bar{\mathbf{k}}(\mathbf{y} - \mathbf{y}^0) + \frac{1}{2}k_{\text{eff}}\lambda^2, \quad (39)$$

where $\bar{\mathbf{k}}$ is the stiffness tensor

$$\bar{\mathbf{k}} = \begin{pmatrix} k_A + k_m & -k_m \\ -k_m & k_B + k_m \end{pmatrix}, \quad (40)$$

k_{eff} is the effective stiffness of the dumbbell as a whole:

$$k_{\text{eff}} = \frac{k_A k_B k_m}{\det(\bar{\mathbf{k}})}, \quad (41)$$

and \mathbf{y}^0 is the vector whose component are the equilibrium positions of the beads:

$$\mathbf{y}^0 = \left(\lambda - \frac{k_B k_m}{\det(\bar{\mathbf{k}})}(\lambda), \frac{k_A k_m}{\det(\bar{\mathbf{k}})}(\lambda) \right). \quad (42)$$

During a pulling experiment the trap to trap distance will be changed at a constant speed, v :

$$\lambda_t = \lambda_0 + vt. \quad (43)$$

As a consequence the equilibrium positions of the beads will change in time:

$$\mathbf{y}^0(t) = \left(\lambda_0 + vt - \frac{k_B k_m}{\det(\bar{\mathbf{k}})}(\lambda_0 + vt), \frac{k_A k_m}{\det(\bar{\mathbf{k}})}(\lambda_0 + vt) \right). \quad (44)$$

During a pulling experiment the free energy of the system changes in time. FRs can be used to determine the free energy change in the system from the distribution of the work performed on the system. As discussed in the main text, the correct definition of the work in such an experiment depends on the way in which the traps are moved. Work is identified as the time derivative of the total potential U :

$$W = -v \int_0^t k_A (y_A(s) - X_A^T(s)) ds \quad (45)$$

Any different definition of work does not yield reliable free energy differences. An alternative work definition can be based on the force measured in the trap at rest (B):

$$W' = v \int_0^t k_B (y_B(s) - X_B^T(s)) ds, \quad (46)$$

a choice made by many experimentalists. Is it possible to infer the distribution of W from the distribution of W' and thus to reliably measure free energy differences? The answer to this is worked out in detail below.

S6.2 W AND W' AS GAUSSIAN RANDOM VARIABLES

In order to answer the questions posed in the previous section we need to study the distributions of W and W' . In this linear model y_A and y_B are Gaussian random variables, so that W and W' , being linear in y_A and y_B , are themselves Gaussian random variables too. The distribution of a Gaussian random variable is determined by its mean and variance. The computation of the mean and variance of the work requires the solution of a system of linear differential equations that can be obtained from the Markov Generator for the joint process (\mathbf{y}, \mathbf{W}) or equivalently from the corresponding Fokker-Planck equation. Here by \mathbf{y} we denote the usual vector containing the positions of the beads while $\mathbf{W} = (v \int_0^t f_A(s) ds, v \int_0^t f_B(s) ds)$. We use the vector \mathbf{W} from which the random variables W, W' are obtained as:

$$W = \mathbf{W}_A, \quad W' = -\mathbf{W}_B. \quad (47)$$

Just as we did when discussing the measurement of hydrodynamic parameters we will use Langevin equations to describe the dynamics of our system:

$$\dot{\mathbf{y}} = -\bar{\mu} \bar{\mathbf{k}} (\mathbf{y} - \mathbf{y}^0) + \eta, \quad (48)$$

where $\bar{\mu}$ is the mobility tensor, describing both friction and hydrodynamic interactions:

$$\bar{\mu} = \begin{pmatrix} \gamma^{-1} & \Gamma^{-1} \\ \Gamma^{-1} & \gamma^{-1} \end{pmatrix}, \quad (49)$$

and η is a white noise compatible with the fluctuation-dissipation theorem, i.e. $\langle \eta_t \eta_s \rangle = 2\beta^{-1} \bar{\mu} \delta(t - s)$. In this setting the Markov generator L for the process (\mathbf{y}, \mathbf{W}) is given by:

$$\begin{aligned} Lf(\mathbf{y}, \mathbf{W}) &= \\ &= (-\bar{\mu} \bar{\mathbf{k}} (\mathbf{y} - \mathbf{y}^0) \cdot \nabla_y + \beta^{-1} \bar{\mu} \cdot \nabla_y \nabla_y - v \bar{\mathbf{k}}_D (\mathbf{y} - \mathbf{X}^T) \cdot \nabla_w) f(\mathbf{y}, \mathbf{W}), \end{aligned} \quad (50)$$

where

$$\bar{\mathbf{k}}_D = \begin{pmatrix} k_A & 0 \\ 0 & k_B \end{pmatrix}. \quad (51)$$

We recall that the Markov generator is the infinitesimal evolution operator in the sense that:

$$\frac{\partial}{\partial t} \langle f(\mathbf{y}(t), \mathbf{W}(t)) \rangle_y = \langle Lf(\mathbf{y}(t), \mathbf{W}(t)) \rangle_y, \quad (52)$$

where $\langle \rangle_y$ denotes average conditioned to initial condition $(y, 0)$. Applying the Markov Generator to $\mathbf{y}, (\mathbf{y} - \langle \mathbf{y} \rangle_y) \otimes (\mathbf{y} - \langle \mathbf{y} \rangle_y), \mathbf{W}, (\mathbf{W} - \langle \mathbf{W} \rangle_y) \otimes (\mathbf{W} - \langle \mathbf{W} \rangle_y)$ ¹ and then taking the average, we obtain the

¹ $\mathbf{i} \otimes \mathbf{j}$ denotes the tensor $\bar{\mathbf{J}}$ such that $\bar{\mathbf{J}} \mathbf{k} = (\mathbf{i} \cdot \mathbf{k}) \mathbf{j}$.

equations of motion for $\langle \mathbf{y} \rangle_y$, $\bar{\sigma}_y^2 = \langle (\mathbf{y} - \langle \mathbf{y} \rangle_y) \otimes (\mathbf{y} - \langle \mathbf{y} \rangle_y) \rangle_y$, $\langle \mathbf{W} \rangle_y$, $\bar{\mathbf{C}} = \langle (\mathbf{W} - \langle \mathbf{W} \rangle_y) \otimes (\mathbf{y} - \langle \mathbf{y} \rangle_y) \rangle_y$ and $\bar{\sigma}_W^2 = \langle (\mathbf{W} - \langle \mathbf{W} \rangle_y) \otimes (\mathbf{W} - \langle \mathbf{W} \rangle_y) \rangle_y$.

$$\frac{d}{dt} \langle \mathbf{y} \rangle_y = -\bar{\mu} \bar{\mathbf{k}} (\langle \mathbf{y} \rangle_y - \mathbf{y}^0(t)) \quad (53)$$

$$\frac{d}{dt} \bar{\sigma}_y^2 = -2\text{Sym} \left(\bar{\mu} \bar{\mathbf{k}} \bar{\sigma}_y^2 + \frac{\bar{\mu}}{\beta} \right) \quad (54)$$

$$\frac{d}{dt} \langle \mathbf{W} \rangle_y = -\bar{\mathbf{k}}_D (\langle \mathbf{y} \rangle_y - \mathbf{X}^T(t)) \quad (55)$$

$$\frac{d}{dt} \bar{\mathbf{C}} = -\bar{\mu} \bar{\mathbf{k}} \bar{\mathbf{C}} - \bar{\sigma}_y^2 \bar{\mathbf{k}}_D \quad (56)$$

$$\frac{d}{dt} \bar{\sigma}_W^2 = -2\bar{\mathbf{k}}_D \bar{\mathbf{C}}, \quad (57)$$

where $\text{Sym}(\cdot)$ in (54) is the operator which gives the symmetric part of its argument. These equations are explicitly derived in subsection S6.5 and solved in subsection S6.6, while we shall now comment on the result.

The calculations reported in the next sections show that, after neglecting transients:

$$\langle \mathbf{W}(t) \rangle = -v \int_0^t \bar{\mathbf{k}}_D (\mathbf{y}^0(s) - \mathbf{X}^T(s)) ds + \bar{\mathbf{k}}_D \bar{\mathbf{k}}^{-1} \bar{\mu}^{-1} \bar{\mathbf{k}}^{-1} \bar{\mathbf{k}}_D \dot{\mathbf{X}}^T v t, \quad (58)$$

and

$$\bar{\sigma}_W^2 = 2 \frac{\bar{\mathbf{k}}_D \bar{\mathbf{k}}^{-1} \bar{\mu}^{-1} \bar{\mathbf{k}}^{-1} \bar{\mathbf{k}}_D}{\beta} v^2 t \quad (59)$$

The first term on the right hand side of (58) is the integral:

$$v \bar{\mathbf{k}}_D \left(\int_0^t -(\mathbf{y}^0(s) - \mathbf{X}^T(s)) ds \right), \quad (60)$$

the difference $\bar{\mathbf{k}}_D(\mathbf{y}^0(s) - \mathbf{X}^T(s))$ gives the equilibrium force in each trap at time s , this is just the force that would be obtained at the corresponding trap-to-trap distance λ if the pulling were carried out reversibly. The two components of the vector $\bar{\mathbf{k}}_D \left(\int_0^t (\mathbf{y}^0(s) - \mathbf{X}^T(s)) ds \right)$ are of course equal in size but different in sign:

$$v \bar{\mathbf{k}}_D \left(\int_0^t -(\mathbf{y}^0(s) - \mathbf{X}^T(s)) ds \right) = \left(v \int_0^t f_{\text{rev}}(s) ds, -v \int_0^t f_{\text{rev}}(s) ds \right). \quad (61)$$

The above expression is then just the reversible work:

$$W_{\text{rev}} = k_{\text{eff}} \left(\lambda_0 v t + \frac{1}{2} v^2 t^2 \right). \quad (62)$$

where we used Eqs.(39) and (43). The second term in (58) is the dominant non-equilibrium contribution (by the way, this is the only term which is linear in time), which arises from the finite pulling speed of the protocol. A key element in this dissipation term is:

$$\bar{\Omega} = \bar{\mathbf{k}}_D \bar{\mathbf{k}}^{-1} \bar{\mu}^{-1} \bar{\mathbf{k}}^{-1} \bar{\mathbf{k}}_D = \bar{\mathbf{p}}^T \bar{\mu}^{-1} \bar{\mathbf{p}}. \quad (63)$$

To give some insight on the physical meaning of this quantity we note that $\bar{\mathbf{p}}$ transforms the trap position vector \mathbf{X}^T into the equilibrium position vector \mathbf{y}^0 :

$$\mathbf{y}^0 = \bar{\mathbf{p}} \mathbf{X}^T. \quad (64)$$

This dissipation term stems from friction ($\bar{\mu}^{-1}$), the relevant velocity being that of the equilibrium positions of the beads. The same element $\bar{\Omega}$ appears in the variance. Now, coming to W and W' we have:

$$\langle W \rangle = W_{\text{rev}} + \bar{\Omega}_{AA} v^2 t \quad (65)$$

$$\sigma_W^2 = \frac{2}{\beta} \bar{\Omega}_{AA} v^2 t \quad (66)$$

$$\langle W' \rangle = W_{\text{rev}} - \bar{\Omega}_{AB} v^2 t \quad (67)$$

$$\sigma_{W'}^2 = \frac{2}{\beta} \bar{\Omega}_{BB} v^2 t. \quad (68)$$

Based on these expressions we introduce the asymmetry factor:

$$\text{AF} = \frac{\sigma_W^2 - \sigma_{W'}^2}{\langle W \rangle - \langle W' \rangle}. \quad (69)$$

This quantity relates the distribution of W to W' based on equilibrium information. The AF does not depend either on the pulling speed, which is evident from Eqs. (65),(66),(67),(68) or on the hydrodynamic parameters. An explicit computation gives:

$$\text{AF} = \frac{1}{\beta} \frac{4k_m(k_A - k_B)}{k_A(k_B + 2k_m)}. \quad (70)$$

S6.3 THE AF CAN BE MEASURED FROM EQUILIBRIUM FORCE TRACES

The AF can be directly measured from the equilibrium force traces. The equilibrium distribution for bead positions follows the Boltzmann distribution with respect to the potential in Eq.(39), i.e.

$$P(\mathbf{y}) = Z^{-1} \exp \left(-\frac{\beta}{2} (\mathbf{y} - \mathbf{y}^0) \cdot \bar{\mathbf{k}} (\mathbf{y} - \mathbf{y}^0) \right), \quad (71)$$

According to such distribution variance of \mathbf{y} is:

$$\text{var}(\mathbf{y}) = \beta^{-1} \bar{\mathbf{k}}^{-1}. \quad (72)$$

Moreover, since forces and bead positions are linearly related, $\mathbf{f} = \bar{\mathbf{k}}_D (\mathbf{y} - \mathbf{X}^T)$ we have:

$$\beta \text{var}(\mathbf{f}) = \bar{\mathbf{k}}_D \bar{\mathbf{k}}^{-1} \bar{\mathbf{k}}_D = \frac{1}{k_A k_B + k_m k_A + k_m k_B} \begin{pmatrix} k_A^2 (k_B + k_m) & k_A k_B k_m \\ k_A k_B k_m & k_B^2 (k_A + k_m) \end{pmatrix}, \quad (73)$$

where $\beta = (K_B T)^{-1}$. Using this formula we get:

$$k_A = \beta \text{var}(\mathbf{f})_{AA} + \beta \text{var}(\mathbf{f})_{AB} \quad (74)$$

$$k_B = \beta \text{var}(\mathbf{f})_{BB} + \beta \text{var}(\mathbf{f})_{AB} \quad (75)$$

$$k_m = k_A k_B \frac{\text{var}(\mathbf{f})_{AB}}{\beta \det(\text{var}(\mathbf{f}))}. \quad (76)$$

These formulas assume that the dynamics of the dumbbell is strictly one-dimensional and takes place in the optical plane, i.e. that plane perpendicular to the optical axis. If this is not the case this simplified treatment is not valid anymore and out-of-plane fluctuations must be taken into account. A discussion of these effects can be found in [1]. Once k_A, k_B and k_m are known the AF can be easily computed by Eq. (70). The present method for measuring rigidities from equilibrium force traces was applied and discussed in detail, in a totally different context, in Reference [2]. We used it in this study to extract the values of k_A, k_B, k_m for the asymmetric setup.

S6.4 DERIVATION OF THE EXPRESSION FOR THE AF

The AF, as given in Eq. (70), can be obtained once the elements of $\bar{\Omega}$ are known. We start from the definition of $\bar{\Omega}$:

$$\bar{\Omega} = \bar{\mathbf{p}}^T \bar{\mu}^{-1} \bar{\mathbf{p}}, \quad (77)$$

where

$$\bar{\mathbf{p}} = \bar{\mathbf{k}}^{-1} \bar{\mathbf{k}}_D = \frac{1}{\mathcal{E}} \begin{pmatrix} k_A(k_B + k_m) & k_B k_m \\ k_A k_m & k_B(k_A + k_m) \end{pmatrix}, \quad (78)$$

with $\mathcal{E} = k_A k_B + k_A k_m + k_B k_m$. Here it is useful to switch to a representation in which $\bar{\mu}^{-1}$ is diagonal. This can be achieved with a $\pi/4$ rotation:

$$\bar{\mathbf{R}} = \frac{1}{\sqrt{2}} \begin{pmatrix} 1 & -1 \\ 1 & 1 \end{pmatrix}. \quad (79)$$

Using $\bar{\mathbf{R}}$ we can write:

$$\bar{\Omega} = \bar{\mathbf{p}}^T \bar{\mathbf{R}} \bar{\mathbf{R}}^T \bar{\mu}^{-1} \bar{\mathbf{R}} \bar{\mathbf{R}}^T \bar{\mathbf{p}}, \quad (80)$$

where, as in Section S1, $\bar{\mathbf{R}}^T \bar{\mu}^{-1} \bar{\mathbf{R}}$ is diagonal. The nontrivial contribution which must still be computed is:

$$\bar{\mathbf{p}}' = \bar{\mathbf{R}}^T \bar{\mathbf{p}} = \frac{1}{\sqrt{2}\mathcal{E}} \begin{pmatrix} k_A(k_B + 2k_m) & k_B(k_A + 2k_m) \\ -k_A k_m & k_B k_A \end{pmatrix} = \frac{1}{\sqrt{2}\mathcal{E}} \begin{pmatrix} A & B \\ -C & C \end{pmatrix}. \quad (81)$$

We can thus conclude that:

$$\bar{\Omega} = \frac{1}{2\mathcal{E}^2} \begin{pmatrix} A & -C \\ B & C \end{pmatrix} \begin{pmatrix} \gamma_+ A & \gamma_+ B \\ -\gamma_- C & \gamma_- C \end{pmatrix} = \frac{1}{2\mathcal{E}^2} \begin{pmatrix} \gamma_+ A^2 + \gamma_- C^2 & \gamma_+ AB - \gamma_- C^2 \\ \gamma_+ AB - \gamma_- C^2 & \gamma_+ B^2 + \gamma_- C^2 \end{pmatrix}. \quad (82)$$

By definition we have:

$$AF = \frac{2\bar{\Omega}_{AA} - \bar{\Omega}_{BB}}{\beta\bar{\Omega}_{AA} + \bar{\Omega}_{AB}} = \frac{2}{\beta} \frac{A - B}{A} = \frac{1}{\beta} \frac{4k_m(k_A - k_B)}{k_A(k_B + 2k_m)}. \quad (83)$$

S6.5 DERIVATION OF THE EQUATIONS

In order to derive the equations of motion (53)-(57) we must apply the Markov Generator to the proper quantities, recalling that

$$\frac{d}{dt} \langle f(\mathbf{y}(t), \mathbf{W}(t)) \rangle_y = \langle Lf(\mathbf{y}(t), \mathbf{W}(t)) \rangle_y. \quad (84)$$

We start by deriving Eq.(53). In this case we have that only the first term in the generator Eq.(50) contributes as the second and third terms involve higher derivatives or derivatives with respect to \mathbf{W} . We conclude that:

$$\frac{d}{dt} \langle \mathbf{y}(t) \rangle_y = \langle L\mathbf{y}(t) \rangle_y = -\bar{\mu} \bar{\mathbf{k}} (\langle \mathbf{y}(t) \rangle_y - \mathbf{y}^0(t)). \quad (85)$$

In the same way we can derive the equation for $\bar{\sigma}_y^2$, it is useful to recall that

$$\langle (\mathbf{y} - \langle \mathbf{y} \rangle_y) \otimes (\mathbf{y} - \langle \mathbf{y} \rangle_y) \rangle_y = \langle \mathbf{y} \otimes \mathbf{y} \rangle_y - \langle \mathbf{y} \rangle_y \otimes \langle \mathbf{y} \rangle_y, \quad (86)$$

so that

$$\frac{d}{dt} \bar{\sigma}_y^2 = \langle L(\mathbf{y} \otimes \mathbf{y}) \rangle_y - \frac{d}{dt} \langle \mathbf{y} \rangle_y \otimes \langle \mathbf{y} \rangle_y \quad (87)$$

we will work out the two terms of the right hand side of (87) separately, starting from the first:

$$\langle L(\mathbf{y} \otimes \mathbf{y}) \rangle_y = \langle (-\bar{\mu} \bar{\mathbf{k}} (\mathbf{y} - \mathbf{y}^0) \cdot \nabla_y + \beta^{-1} \bar{\mu} \cdot \nabla_y \nabla_y) \mathbf{y} \otimes \mathbf{y} \rangle_y. \quad (88)$$

The third term in the generator was neglected because it involves a derivative with respect to \mathbf{W} . Acting with the derivatives on $\mathbf{y} \otimes \mathbf{y}$ gives:

$$\begin{aligned} \langle L(\mathbf{y} \otimes \mathbf{y}) \rangle_y &= -\langle \bar{\mu} \bar{\mathbf{k}} ((\mathbf{y} - \mathbf{y}^0) \otimes \mathbf{y}) - (\mathbf{y} \otimes (\mathbf{y} - \mathbf{y}^0)) (\bar{\mu} \bar{\mathbf{k}})^T \rangle_y + 2\beta^{-1} \bar{\mu} \\ &= -2\text{Sym}(\langle \bar{\mu} \bar{\mathbf{k}} ((\mathbf{y} - \mathbf{y}^0) \otimes \mathbf{y}) \rangle_y) + 2\beta^{-1} \bar{\mu}. \end{aligned} \quad (89)$$

The second term in (87) is just a time derivative, which can be worked out thanks to (85):

$$\begin{aligned} \frac{d}{dt} \langle \mathbf{y} \rangle_y \otimes \langle \mathbf{y} \rangle_y &= -\bar{\mu} \bar{\mathbf{k}} ((\langle \mathbf{y} \rangle_y - \mathbf{y}^0) \otimes \langle \mathbf{y} \rangle_y) - (\langle \mathbf{y} \rangle_y \otimes (\langle \mathbf{y} \rangle_y - \mathbf{y}^0)) (\bar{\mu} \bar{\mathbf{k}})^T = \\ &= -2\text{Sym}(\bar{\mu} \bar{\mathbf{k}} ((\langle \mathbf{y} \rangle_y - \mathbf{y}^0) \otimes \mathbf{y})) . \end{aligned} \quad (90)$$

An explicit result for the time derivative of $\bar{\sigma}_y^2$ is obtained by taking the difference of (89) and (90)

$$\begin{aligned} \frac{d}{dt} \bar{\sigma}_y^2 &= -2\text{Sym}(\langle \bar{\mu} \bar{\mathbf{k}} ((\mathbf{y} - \mathbf{y}^0) \otimes \mathbf{y}) \rangle_y - \bar{\mu} \bar{\mathbf{k}} ((\langle \mathbf{y} \rangle_y - \mathbf{y}^0) \otimes \langle \mathbf{y} \rangle_y)) + 2\beta^{-1} \bar{\mu} = \\ &= -2\text{Sym}(\langle \bar{\mu} \bar{\mathbf{k}} (\mathbf{y} \otimes \mathbf{y}) \rangle_y - \bar{\mu} \bar{\mathbf{k}} (\langle \mathbf{y} \rangle_y \otimes \langle \mathbf{y} \rangle_y)) + 2\beta^{-1} \bar{\mu} = \\ &= -2\text{Sym}(\bar{\mu} \bar{\mathbf{k}} \bar{\sigma}_y^2) + 2\beta^{-1} \bar{\mu} . \end{aligned} \quad (91)$$

In the second step above we used the fact that

$$\langle ((\mathbf{y} - \mathbf{y}^0) \otimes \mathbf{y}) \rangle_y = \langle (\mathbf{y} \otimes \mathbf{y}) \rangle_y - (\mathbf{y}^0 \otimes \langle \mathbf{y} \rangle_y)$$

while

$$((\langle \mathbf{y} \rangle_y - \mathbf{y}^0) \otimes \langle \mathbf{y} \rangle_y) = (\langle \mathbf{y} \rangle_y \otimes \langle \mathbf{y} \rangle_y) - (\mathbf{y}^0 \otimes \langle \mathbf{y} \rangle_y) .$$

Following the order of equations (53)-(57) we should now compute the average of \mathbf{W} . This is again a simple matter, as the computation proceeds almost exactly as in the case of $\langle \mathbf{y} \rangle_y$, with the only difference that now only the last term in Eq.(50) for the generator matters. The result is:

$$\frac{d}{dt} \langle \mathbf{W} \rangle_y = v \bar{\mathbf{k}}_D (\langle \mathbf{y} \rangle_y - \mathbf{X}^T(t)) . \quad (92)$$

The case of $\bar{\mathbf{C}}$, the cross-correlation of \mathbf{y} and \mathbf{W} involves some additional computations. The function $\bar{\mathbf{C}}$ is linear in both \mathbf{W} and \mathbf{y} so that only the first and third terms in the generator contribute. The time derivative of $\bar{\mathbf{C}} = (\mathbf{W} - \langle \mathbf{W} \rangle_y) \otimes (\mathbf{y} - \langle \mathbf{y} \rangle_y)$ again yields two pieces, as in the case of (87), and we shall proceed in a similar way:

$$\frac{d}{dt} \bar{\mathbf{C}} = \langle L(\mathbf{W} \otimes \mathbf{y}) \rangle_y - \frac{d}{dt} \langle \mathbf{W} \rangle_y \otimes \langle \mathbf{y} \rangle_y . \quad (93)$$

Again we will compute the two parts separately:

$$\begin{aligned} \langle L(\mathbf{W} \otimes \mathbf{y}) \rangle_y &= \langle -(\mathbf{W} \otimes (\bar{\mu} \bar{\mathbf{k}}(\mathbf{y} - \mathbf{y}^0))) + ((v \bar{\mathbf{k}}_D(\mathbf{y} - \mathbf{X}^T)) \otimes \mathbf{y}) \rangle_y = \\ &= \langle -\bar{\mu} \bar{\mathbf{k}} (\mathbf{W} \otimes (\mathbf{y} - \mathbf{y}^0)) + v ((\mathbf{y} - \mathbf{X}^T) \otimes \mathbf{y}) \bar{\mathbf{k}}_D \rangle_y , \end{aligned} \quad (94)$$

and

$$\frac{d}{dt} \langle \mathbf{W} \rangle_y \otimes \langle \mathbf{y} \rangle_y = -\bar{\mu} \bar{\mathbf{k}} (\langle \mathbf{W} \rangle_y \otimes (\langle \mathbf{y} \rangle_y - \mathbf{y}^0)) + v ((\langle \mathbf{y} \rangle_y - \mathbf{y}^0) \otimes \langle \mathbf{y} \rangle_y) \bar{\mathbf{k}}_D . \quad (95)$$

Taking the difference of these two terms and using

$$\langle (\mathbf{W} \otimes (\mathbf{y} - \mathbf{y}^0)) \rangle_y = \langle (\mathbf{W} \otimes \mathbf{y}) \rangle_y - (\langle \mathbf{W} \rangle_y \otimes \mathbf{y}^0)$$

and

$$(\langle \mathbf{W} \rangle_y \otimes (\langle \mathbf{y} \rangle_y - \mathbf{y}^0)) = (\langle \mathbf{W} \rangle_y \otimes \langle \mathbf{y} \rangle_y) - (\langle \mathbf{W} \rangle_y \otimes \mathbf{y}^0)$$

it is possible to conclude that:

$$\begin{aligned} \frac{d}{dt} \bar{\mathbf{C}} &= -\bar{\mu} \bar{\mathbf{k}} \langle (\mathbf{W} - \langle \mathbf{W} \rangle_y) \otimes (\mathbf{y} - \langle \mathbf{y} \rangle_y) \rangle_y + \langle (\mathbf{y} - \langle \mathbf{y} \rangle_y) \otimes (\mathbf{y} - \langle \mathbf{y} \rangle_y) \rangle_y \bar{\mathbf{k}}_D \\ &= -\bar{\mu} \bar{\mathbf{k}} \bar{\mathbf{C}} + v \bar{\sigma}_y^2 \bar{\mathbf{k}}_D . \end{aligned} \quad (96)$$

The only equation left to derive is that for $\bar{\sigma}_W^2 = \langle (\mathbf{W} - \langle \mathbf{W} \rangle_y) \otimes (\mathbf{W} - \langle \mathbf{W} \rangle_y) \rangle_y$. This computation will only involve the last term in the generator:

$$\frac{d}{dt} \langle (\mathbf{W} - \langle \mathbf{W} \rangle_y) \otimes (\mathbf{W} - \langle \mathbf{W} \rangle_y) \rangle_y = \langle L(\mathbf{W} \otimes \mathbf{W}) \rangle_y - \frac{d}{dt} (\langle \mathbf{W} \rangle_y \otimes \langle \mathbf{W} \rangle_y) . \quad (97)$$

As usual we will evaluate the two terms separately and put them together as a second step:

$$\langle L(\mathbf{W} \otimes \mathbf{W}) \rangle_y = v \bar{\mathbf{k}}_D (\mathbf{W} \otimes (\mathbf{y} - \mathbf{X}^T)) + ((\mathbf{y} - \mathbf{X}^T) \otimes \mathbf{W}) \bar{\mathbf{k}}_D \rangle_y, \quad (98)$$

$$\frac{d}{dt} (\langle \mathbf{W} \rangle_y \otimes \langle \mathbf{W} \rangle_y) = v \bar{\mathbf{k}}_D (\mathbf{W} \otimes (\langle \mathbf{y} \rangle_y - \mathbf{X}^T)) + ((\langle \mathbf{y} \rangle_y - \mathbf{X}^T) \otimes \mathbf{W}) \bar{\mathbf{k}}_D. \quad (99)$$

The last equation of motion is thus:

$$\begin{aligned} \frac{d}{dt} \bar{\sigma}_W^2 &= +v \bar{\mathbf{k}}_D \langle (\mathbf{y} - \langle \mathbf{y} \rangle_y) \otimes (\mathbf{W} - \langle \mathbf{W} \rangle_y) \rangle_y + v \langle (\mathbf{W} - \langle \mathbf{W} \rangle_y) \otimes (\mathbf{y} - \langle \mathbf{y} \rangle_y) \rangle_y \bar{\mathbf{k}}_D = \\ &= +2\text{Sym}(v \bar{\mathbf{k}}_D \bar{\mathbf{C}}). \end{aligned} \quad (100)$$

S6.6 SOLUTION OF THE EQUATIONS

In the previous section we introduced an average operation $\langle \cdot \rangle_y$ without specifying with respect to which measure the average is taken. In this section we will suppose that the initial probability distribution for the process is $p(\mathbf{y}, 0) = \delta(\mathbf{y} - y)$, a deterministic initial condition. The Work is by definition equal to 0 at $t = 0$, again a deterministic initial condition, and the same is true for the different variances and covariances because of the initial conditions. The initial conditions for the equations of motion will then be:

$$\begin{cases} \langle \mathbf{y}(0) \rangle_y = y \\ \langle \mathbf{W}(0) \rangle_y = \bar{\sigma}_y^2(0) = \bar{\mathbf{C}}(0) = \bar{\sigma}_W^2(0) = 0. \end{cases} \quad (101)$$

All the equations we have to solve are linear equations which can either be solved by variation of constants or by direct integration. The first equation, that for $\langle \mathbf{y} \rangle_y$ is a case for variation of constants:

$$\begin{cases} \langle \mathbf{y}(0) \rangle_y = y \\ \frac{d}{dt} \langle \mathbf{y} \rangle_y = -\bar{\mu} \bar{\mathbf{k}} (\langle \mathbf{y} \rangle_y - \mathbf{y}^0(t)). \end{cases} \quad (102)$$

The solution is

$$\langle \mathbf{y}(t) \rangle_y = e^{-\bar{\mu} \bar{\mathbf{k}} t} \left(y + \int_0^t \bar{\mu} \bar{\mathbf{k}} e^{\bar{\mu} \bar{\mathbf{k}} s} \mathbf{y}^0(s) ds \right), \quad (103)$$

as it can be directly checked. We recall the definition of $\mathbf{y}^0(t)$

$$\mathbf{y}^0(t) = \left(\lambda + vt - \frac{k_A k_m}{\det(\bar{\mathbf{k}})} (\lambda_0 + vt), \frac{k_B k_m}{\det(\bar{\mathbf{k}})} (\lambda_0 + vt) \right). \quad (104)$$

In the following it will be useful to write $\mathbf{y}^0(t) = \psi + \xi t$ where

$$\psi = \left(\lambda_0 - \frac{k_A k_m}{\det(\bar{\mathbf{k}})} \lambda_0, \frac{k_B k_m}{\det(\bar{\mathbf{k}})} \lambda_0 \right) \quad (105)$$

$$\xi = \left(v - \frac{k_A k_m}{\det(\bar{\mathbf{k}})} v, \frac{k_B k_m}{\det(\bar{\mathbf{k}})} v \right). \quad (106)$$

In terms of these quantities (103) reads:

$$\langle \mathbf{y}(t) \rangle_y = e^{-\bar{\mu} \bar{\mathbf{k}} t} \left(y + \int_0^t \bar{\mu} \bar{\mathbf{k}} e^{\bar{\mu} \bar{\mathbf{k}} s} (\psi + \xi s) ds \right). \quad (107)$$

Integrating by parts we get:

$$\begin{aligned}
\langle \mathbf{y}(t) \rangle_y &= e^{-\bar{\mu}\bar{k}t} \left(y + \int_0^t \bar{\mu}\bar{k}e^{\bar{\mu}\bar{k}s}(\psi + \xi t)ds \right) = \\
&= e^{-\bar{\mu}\bar{k}t} \left(y + e^{\bar{\mu}\bar{k}s}(\psi + \xi s) \Big|_0^t - \int_0^t e^{\bar{\mu}\bar{k}s}\xi ds \right) = \\
&= e^{-\bar{\mu}\bar{k}t} \left(y + e^{\bar{\mu}\bar{k}t}(\psi + \xi t) - \psi - (\bar{\mu}\bar{k})^{-1}e^{\bar{\mu}\bar{k}s}\xi \Big|_0^t \right) = \\
&= e^{-\bar{\mu}\bar{k}t} \left(y + e^{\bar{\mu}\bar{k}t}(\psi + \xi t) - (\bar{\mu}\bar{k})^{-1} \left(e^{\bar{\mu}\bar{k}t} - 1 \right) \xi \right) = \\
&= \left(e^{-\bar{\mu}\bar{k}t}(y - \psi) + (\psi + \xi t) - (\bar{\mu}\bar{k})^{-1} \left(1 - e^{-\bar{\mu}\bar{k}t} \right) \xi \right) = \\
&= e^{-\bar{\mu}\bar{k}t}(y - \psi) + \mathbf{y}^0(t) - (\bar{\mu}\bar{k})^{-1} \left(1 - e^{-\bar{\mu}\bar{k}t} \right) \xi
\end{aligned} \tag{108}$$

The average $\langle \mathbf{W} \rangle_y$ is given by:

$$\begin{aligned}
\langle \mathbf{W} \rangle_y &= \bar{k}_D \int_0^t \langle \mathbf{y}(s) \rangle_y - \mathbf{X}^T(s)ds = \\
&= \bar{k}_D \int_0^t e^{-\bar{\mu}\bar{k}s}(y - \psi) + \mathbf{y}^0(s) - (\bar{\mu}\bar{k})^{-1} \left(1 - e^{-\bar{\mu}\bar{k}s} \right) \xi - \mathbf{X}^T(s)ds = \\
&= \bar{k}_D \left(\int_0^t (\mathbf{y}^0(s) - \mathbf{X}^T(s)ds) - (\bar{\mu}\bar{k})^{-1}e^{-\bar{\mu}\bar{k}s}(y - \psi) \Big|_0^t \right. \\
&\quad \left. - (\bar{\mu}\bar{k})^{-1} \left(s + (\bar{\mu}\bar{k})^{-1}e^{-\bar{\mu}\bar{k}s} \right) \Big|_0^t \xi \right) = \\
&= \bar{k}_D \left(\int_0^t (\mathbf{y}^0(s) - \mathbf{X}^T(s)ds) - (\bar{\mu}\bar{k})^{-1} \left(e^{-\bar{\mu}\bar{k}s} - 1 \right) (y - \psi) \right. \\
&\quad \left. + (\bar{\mu}\bar{k})^{-1} \left(t + (\bar{\mu}\bar{k})^{-1} \left(e^{-\bar{\mu}\bar{k}t} - 1 \right) \right) \xi \right)
\end{aligned} \tag{109}$$

The equation for the variance $\bar{\sigma}_y^2$ requires some more attention, we first prove a useful identity: let A and B be symmetric matrices. The product AB is not in general symmetric

$$(AB)^T = BA.$$

As a consequence the exponential of AB , e^{AB} is not symmetric. We want now to prove that:

$$(A^{-1}e^{AB}) = (A^{-1}e^{AB})^T = e^{BA}A^{-1}. \tag{110}$$

Using the definition of the matrix exponential we have:

$$\begin{aligned}
A^{-1}e^{AB} &= A^{-1} \sum_{k=0}^{\infty} \frac{(AB)^k}{k!} = A^{-1} + B + BAB + \dots = (1 + BA + BABA + \dots) A^{-1} \\
&= \sum_{i=0}^{\infty} \frac{(BA)^i}{i!} A^{-1} = e^{BA} A^{-1}.
\end{aligned} \tag{111}$$

Similarly one can prove:

$$(Ae^{AB}) = (Ae^{AB})^T = e^{BA}A. \tag{112}$$

These results will prove useful in solving the equation for $\bar{\sigma}_y^2$. We will first solve:

$$\begin{cases} \bar{\sigma}_y^2(0) = 0 \\ \frac{d}{dt} \bar{\sigma}_y^2 = -2\bar{\mu}\bar{k}\bar{\sigma}_y^2 + 2\frac{\bar{\mu}}{\bar{\beta}}, \end{cases} \tag{113}$$

and then prove that the solution of (113) also solves (54). Equation (113) can again be solved by variation of the constants:

$$\begin{aligned}\bar{\sigma}_y^2(t) &= e^{-2\bar{\mu}\bar{k}t} \int_0^t e^{2\bar{\mu}\bar{k}s} 2\frac{\bar{\mu}}{\beta} ds = e^{-2\bar{\mu}\bar{k}t} \left(e^{2\bar{\mu}\bar{k}s} (\bar{\mu}\bar{k})^{-1} \frac{\bar{\mu}}{\beta} \right) \Big|_0^t = \\ &= \left(1 - e^{-2\bar{\mu}\bar{k}t} \right) \frac{\bar{k}^{-1}}{\beta}.\end{aligned}\tag{114}$$

The original equation for $\bar{\sigma}_y^2$ contains $\text{Sym}(\bar{\mu}\bar{k}\bar{\sigma}_y^2)$. Using (110),(112) we can prove that:

$$\bar{\mu}\bar{k}\bar{\sigma}_y^2(t) = \bar{\mu}\bar{k} \left(1 - e^{-2\bar{\mu}\bar{k}t} \right) \frac{\bar{k}^{-1}}{\beta} = \frac{\bar{k}^{-1}}{\beta} \left(1 - e^{-2\bar{\mu}\bar{k}t} \right)^T k\mu = (\bar{\mu}\bar{k}\bar{\sigma}_y^2(t))^T.\tag{115}$$

In other words

$$\bar{\mu}\bar{k}\bar{\sigma}_y^2(t) = \text{Sym}(\bar{\mu}\bar{k}\bar{\sigma}_y^2(t)),$$

so that if $\bar{\sigma}_y^2(t)$ solves (113) it also solves (54). The equation for \bar{C} , is again solved by variation of constants:

$$\begin{cases} \bar{C}(0) = 0 \\ \frac{d}{dt}\bar{C} = -\bar{\mu}\bar{k}\bar{C} + v\bar{\sigma}_y^2\bar{k}_D. \end{cases}\tag{116}$$

The solution is:

$$\begin{aligned}\bar{C}(t) &= ve^{-\bar{\mu}\bar{k}t} \int_0^t e^{\bar{\mu}\bar{k}s} \bar{\sigma}_y^2(s) \bar{k}_D ds = \\ &= ve^{-\bar{\mu}\bar{k}t} \int_0^t e^{\bar{\mu}\bar{k}s} \left(1 - e^{-2\bar{\mu}\bar{k}s} \right) \frac{\bar{k}^{-1}\bar{k}_D}{\beta} ds = \\ &= ve^{-\bar{\mu}\bar{k}t} \int_0^t \left(e^{\bar{\mu}\bar{k}s} - e^{-\bar{\mu}\bar{k}s} \right) \frac{\bar{k}^{-1}\bar{k}_D}{\beta} ds = \\ &= ve^{-\bar{\mu}\bar{k}t} (\bar{\mu}\bar{k})^{-1} \left(e^{\bar{\mu}\bar{k}s} + e^{-\bar{\mu}\bar{k}s} \right) \Big|_0^t \frac{\bar{k}^{-1}\bar{k}_D}{\beta} = \\ &= ve^{-\bar{\mu}\bar{k}t} (\bar{\mu}\bar{k})^{-1} \left(e^{\bar{\mu}\bar{k}t} + e^{-\bar{\mu}\bar{k}t} - 2 \right) \frac{\bar{k}^{-1}\bar{k}_D}{\beta} = \\ &= v(\bar{\mu}\bar{k})^{-1} \left(1 + e^{-2\bar{\mu}\bar{k}t} - 2e^{-\bar{\mu}\bar{k}t} \right) \frac{\bar{k}^{-1}\bar{k}_D}{\beta} = \\ &= v(\bar{\mu}\bar{k})^{-1} \left(1 - e^{-\bar{\mu}\bar{k}t} \right)^2 \frac{\bar{k}^{-1}\bar{k}_D}{\beta}.\end{aligned}\tag{117}$$

As in the case of $\langle W \rangle_y$ the equation for $\bar{\sigma}_W^2$ is solved by direct integration:

$$\begin{aligned}\bar{\sigma}_W^2 &= \int_0^t 2v^2\bar{k}_D\bar{C}(s)ds = \int_0^t v\bar{k}_D(\bar{\mu}\bar{k})^{-1} \left(1 - e^{-\bar{\mu}\bar{k}s} \right)^2 \frac{\bar{k}^{-1}\bar{k}_D}{\beta} ds = \\ &= 2v^2 \int_0^t \bar{k}_D(\bar{\mu}\bar{k})^{-1} \left(1 - 2e^{-\bar{\mu}\bar{k}s} + e^{-2\bar{\mu}\bar{k}s} \right) \frac{\bar{k}^{-1}\bar{k}_D}{\beta} ds = \\ &= 2v^2\bar{k}_D(\bar{\mu}\bar{k})^{-1} \left(s + 2(\bar{\mu}\bar{k})^{-1}e^{-\bar{\mu}\bar{k}s} - \frac{(\bar{\mu}\bar{k})^{-1}}{2}e^{-2\bar{\mu}\bar{k}s} \right) \Big|_0^t \frac{\bar{k}^{-1}\bar{k}_D}{\beta} = \\ &= 2v^2\bar{k}_D(\bar{\mu}\bar{k})^{-1} \left(t + 2(\bar{\mu}\bar{k})^{-1} \left(e^{-\bar{\mu}\bar{k}t} - 1 \right) - \frac{(\bar{\mu}\bar{k})^{-1}}{2} \left(e^{-2\bar{\mu}\bar{k}t} - 1 \right) \right) \frac{\bar{k}^{-1}\bar{k}_D}{\beta} = \\ &= v^2\bar{k}_D(\bar{\mu}\bar{k})^{-2} \left(2\bar{\mu}\bar{k}t + 2 \left(e^{-\bar{\mu}\bar{k}t} - 1 \right) - \left(e^{-2\bar{\mu}\bar{k}t} - 1 \right) \right) \frac{\bar{k}^{-1}\bar{k}_D}{\beta}\end{aligned}\tag{118}$$

Keeping terms of order $\mathcal{O}(t)$ in Eqs. (108) and (118) we get the expressions anticipated in Eqs. (58) and (59)

S7 EXPERIMENTS AT LOWER PULLING SPEED

In the main text we present experiments performed at high pulling speed, in order to enhance the dissipation associated with the movement of the center-of-mass. This was done to highlight the fact that W' does not fulfill the CFR. Nevertheless such violation is still evident at lower pulling speeds. Just for completeness in figure S7 we show the distributions of W_- , W , W' and W_+ in a pulling experiment performed on a dsDNA tether (experimental conditions are identical to those reported in the main paper) at a pulling speed of 500 nm/s with $\Delta\lambda = 400$ nm.

References

- [1] Ribezzi-Crivellari M, Ritort F (2012) Force spectroscopy with dual-trap optical tweezers: Molecular stiffness measurements and coupled fluctuations analysis. *Biophysical journal* 103:1919–1928.
- [2] Ribezzi-Crivellari M, Ritort F (2013) Counter-propagating dual-trap optical tweezers based on linear momentum conservation *Review of Scientific Instruments* 84:043104
- [3] Batchelor GK (1976) Brownian diffusion of particles with hydrodynamic interaction. *Journal of Fluid Mechanics* 74:1–29.
- [4] Happel J, Brenner H (1991) *Low Reynolds number hydrodynamics: with special applications to particulate media* (Kluwer Academic Print on Demand).

CAPTION FOR FIGURE 1

Experimental set-up. Two laser beams, oriented along the z direction, are used to create two optical traps. A dumbbell is formed by two optically trapped beads and a molecular tether. The tether is oriented along the y direction, perpendicular to the optical axis z . We choose the center of one trap (trap B) as the origin of our coordinate system. λ denotes the trap-to-trap distance while y_A and y_B denote the positions of the centers of the beads with respect to the reference trap B.

CAPTION FOR FIGURE 2

Independent coordinates in linear systems A) Two dimensional histograms of the forces measured in a **symmetric** dual trap setup. The dashed line forms a $\pi/4$ angle with the coordinate axes and corresponds to the definition of f_+ . B) Covariance $\langle f_+^\phi f_-^\phi \rangle$ as a function of ϕ in a symmetric setup. The red line denotes 0 covariance (i.e. linear independence). At the bottom of the graph we report the result of a 1% significance χ^2 test, with red meaning dependent and green meaning independent. C) Two dimensional histograms of the force as measured in an **asymmetric** dual trap setup. The dashed line forms a $\pi/4$ angle with the coordinate axes and corresponds to the definition of f_+ . In this asymmetric case f_+ , f_- do not correspond to the principal axes of the histogram. D) Covariance $\langle f_+^\phi f_-^\phi \rangle$ as a function of ϕ in a **asymmetric** setup. The red line denotes 0 covariance (i.e. linear independence). It is still possible to define a coordinate system where the two degrees of freedom are uncoupled, but now the definition is different from that given in the main text. At the bottom of the graph we report the result of a 1% significance χ^2 test, with red meaning dependent and green meaning independent. Tests were performed on 3 seconds data traces with 1kHz acquisition rate.

CAPTION FOR FIGURE 3

Independent coordinates in non-linear systems Left panels: force fluctuations of a two-state DNA hairpin. Force increases from top to bottom and the hairpin is 1) completely folded, 2) preferentially folded, 3) preferentially unfolded, 4) completely unfolded. Right panels: Covariance $\langle f_+^\phi f_-^\phi \rangle$ as a function of ϕ . The red line denotes 0 covariance (i.e. linear independence). At the bottom of the graphs we report

the result of a 1% significance χ^2 test, with red meaning dependent and green meaning independent. Data show that the center of mass (x_+) and differential coordinate (x_-) are independent. Tests were performed on 3 seconds data traces with 1kHz acquisition rate.

CAPTION FOR FIGURE 4

Direct measurements γ and Γ . Left panel: hydrodynamic friction (γ , solid symbols) and interaction coefficient (Γ , open symbols) measured from the decay rate of thermal fluctuations. Each point is the average upon measurements over 5 different molecules. Solid lines are the theoretical predictions Eqs. (31),(32). The horizontal dashed line marks the exact theoretical value at contact ($\rho = 2$). Right panel: Ratio between the hydrodynamic coefficients (Γ/γ) as a function of $(\rho - 2)^{-1}$. This quantity does not depend directly on r_b . Open symbols represent measurements obtained with untethered beads at different separations, solid symbols show measurements obtained with tethered beads. The continuous line gives the theoretical prediction according to the first two term in the expansion as in Eqs. (31),(32).

CAPTION FOR FIGURE 5

Convolution and reconstruction of $P(W)$ from the CFR for the asymmetric case. Each row shows the result of a convolution by fixing the value of Σ and changing Δ . The top, middle and bottom rows correspond to $\Sigma^2 = 0, \Sigma^2 = 2.5, \Sigma^2 = 7.5$. In each panel we show $P_{\Delta,\Sigma}(W)$ (blue solid points), together with $P_{\Delta,\Sigma}(-W)\exp(W)$ (blue open points) and the experimentally measured $P(W)$ (green points). Three different convolutions are found to fulfill the fluctuation symmetry $P_{\Delta,\Sigma}(W) = P_{\Delta,\Sigma}(-W)\exp(W)$, (panels in the rightmost column), but only one of them (bottom right panel) is compatible with the AF and matches the true $P(W)$.

CAPTION FOR FIGURE 6

Asymmetry factor and inference in asymmetric setups Left panel: The asymmetry factor as a function of k_A/k_B and k_m/k_B . Different curves correspond to different values of k_m/k_B (0.3,0.5,1,2,3 from bottom to top). The dashed curve corresponds to the limit $k_m = \infty$. In the symmetric case ($k_A = k_B = 1$) the different curves coincide ($\Sigma^2 = 0$). The red point denotes the asymmetric conditions in which experiments were performed. Right panel: Inference in the asymmetric case. Different pairs (Δ, Σ^2) yield probability distributions satisfying the CFR (blue points and blue line). The asymmetry factor (red line) selects a narrow range of possible values, which is compatible with the experimentally measured values $\Delta = 8.2 K_B T$ and $\Sigma^2 = 7.2 (K_B T)^2$.

CAPTION FOR FIGURE 7

Work measurements at lower pulling speed. The statistics of W, W', W_+ and W_- are shown. The pulling speed $v = 500$ nm/s is less than half of the lowest pulling speed presented in the main text, but the effect on the validity of the CFR for the different work quantities (W, W', W^+, W^-) is still visible. 500 nm/s lies in the typical range of pulling speed used in single molecule pulling experiments.

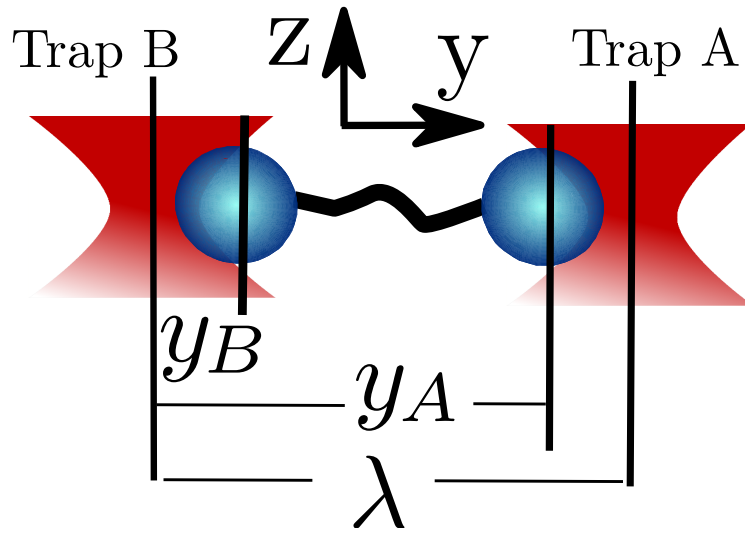


Figure S 1

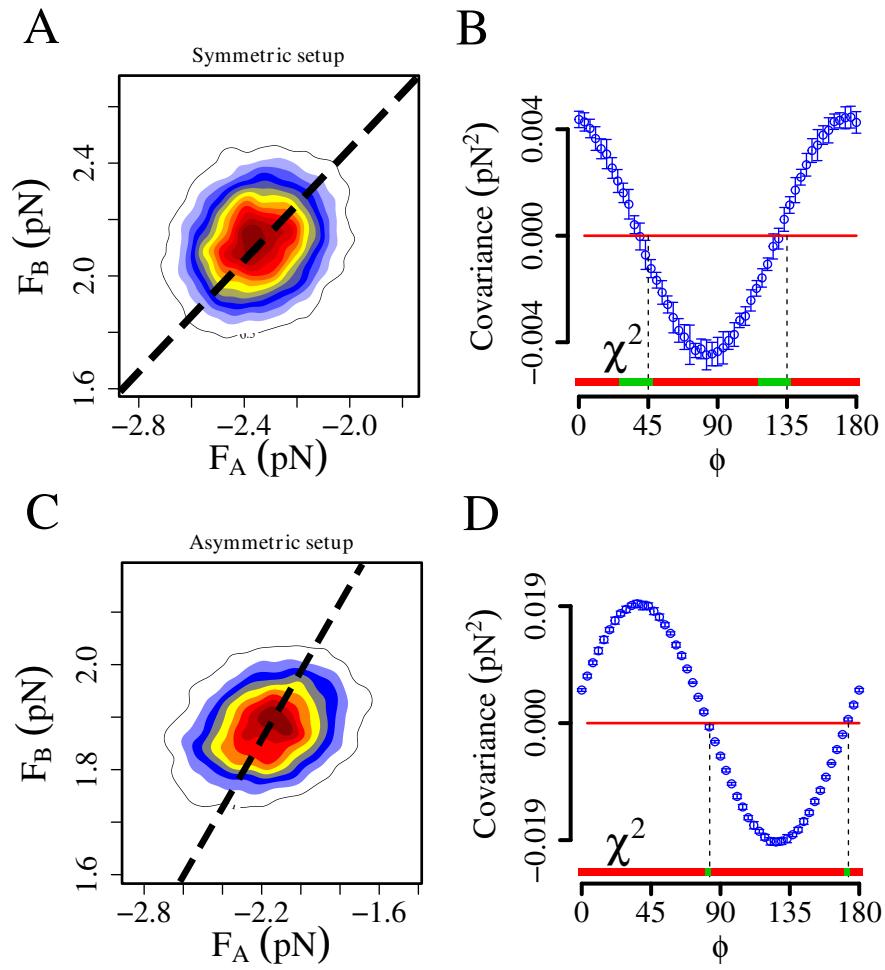


Figure S 2

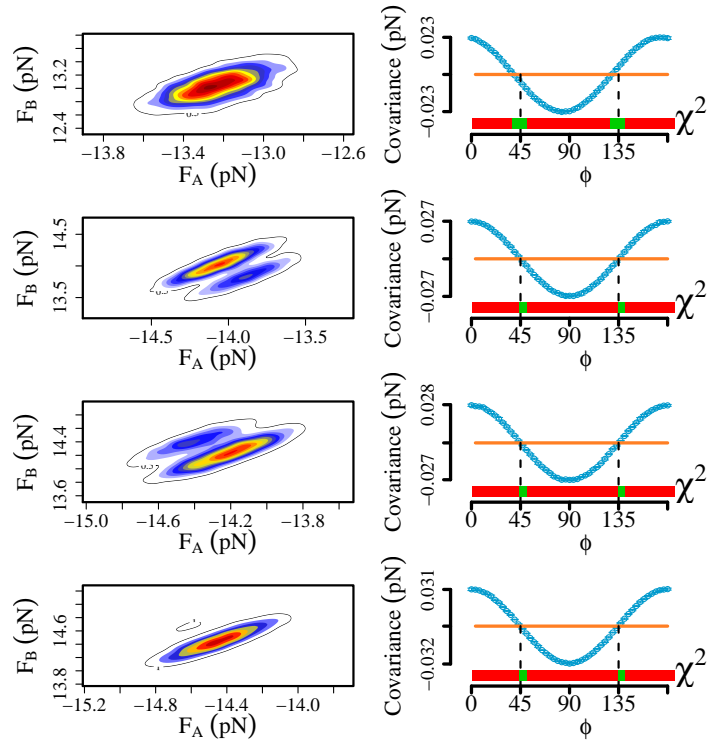


Figure S 3

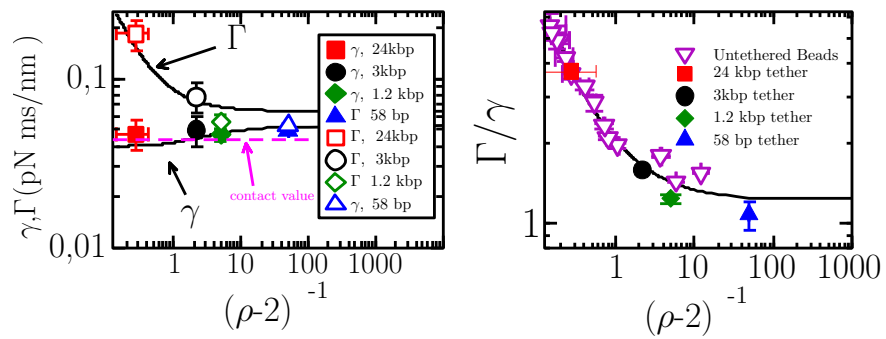


Figure S 4

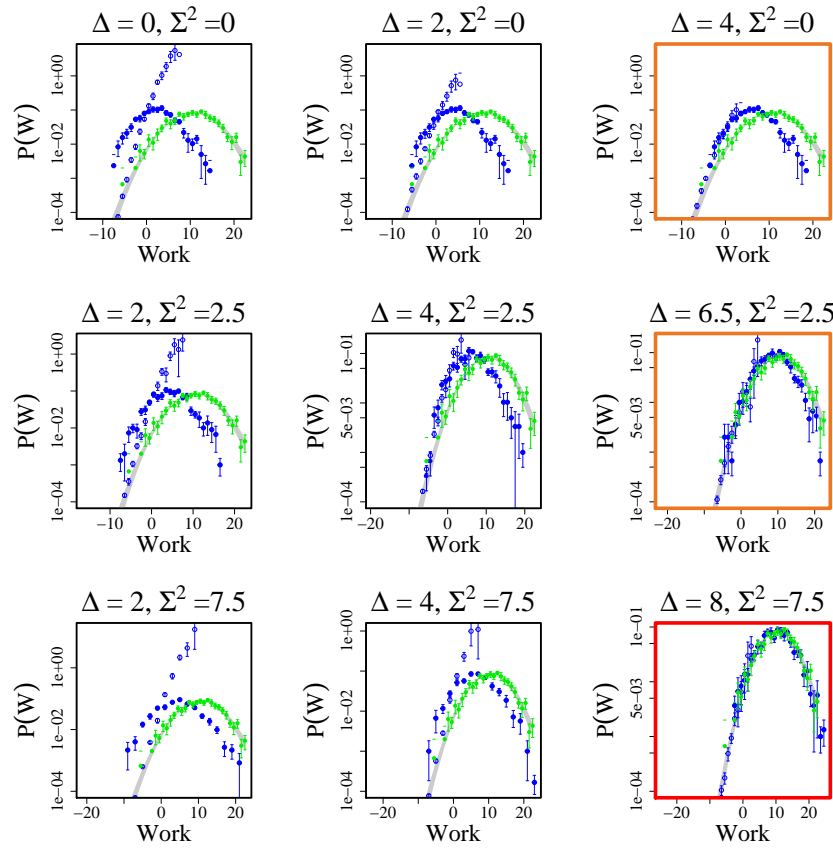


Figure S 5

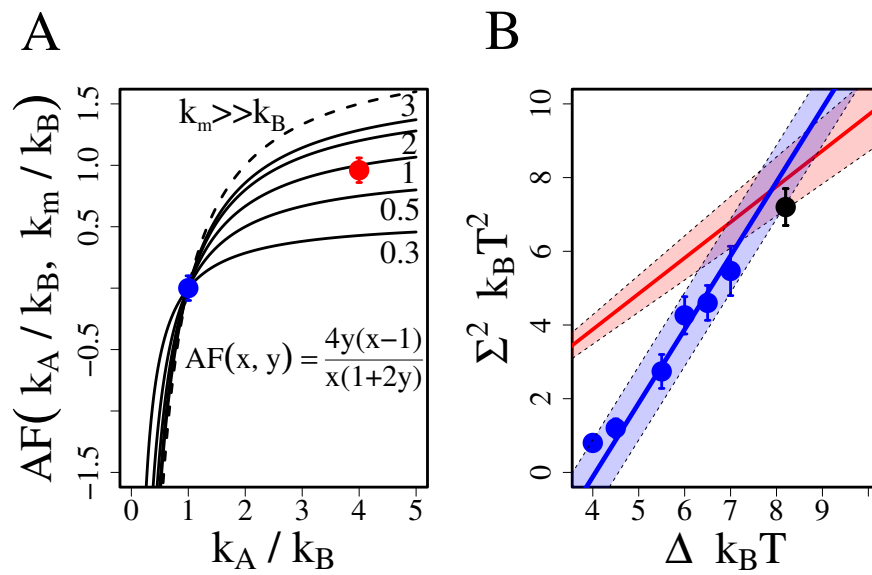


Figure S 6

$v=500$ nm/s

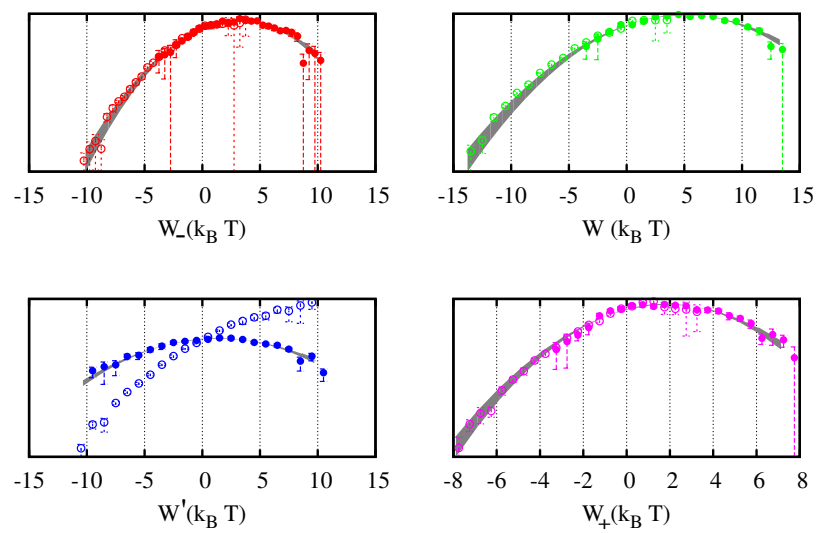


Figure S 7

TABLE S1

Table S 1: Molecule 1

Pulling speed	cov(W, W')	χ^2 -test ¹	cov(W^+, W^-)	χ^2 -test ¹
Forward protocol				
7.2 $\mu\text{m/s}$	0.41	1	0.08	0
4.3 $\mu\text{m/s}$	0.35	1	0.09	0
1.35 $\mu\text{m/s}$	0.38	1	0.05	0
Reverse protocol				
7.2 $\mu\text{m/s}$	0.17	0	0.018	0
4.3 $\mu\text{m/s}$	-0.05	0	-0.05	0
1.35 $\mu\text{m/s}$	0.36	1	0.20	0
Cyclic protocol				
7.2 $\mu\text{m/s}$	0.12	1	0.00	0
4.3 $\mu\text{m/s}$	0.12	1	0.01	0
1.35 $\mu\text{m/s}$	0.34	1	0.09	0

¹ 1=Dependent 0=Independent

TABLE S2

Table S 2: Molecule 2

Pulling speed	cov(W, W')	χ^2 -test ¹	cov(W^+, W^-)	χ^2 -test ¹
Forward protocol				
7.2 $\mu\text{m/s}$	0.469377	1	-0.12	1
4.3 $\mu\text{m/s}$	0.6170601	1	-0.14	0
1.35 $\mu\text{m/s}$	0.5346567	1	0.09	0
Reverse protocol				
7.2 $\mu\text{m/s}$	-0.31	1	0.25	0
4.3 $\mu\text{m/s}$	-0.37	1	0.20	0
1.35 $\mu\text{m/s}$	-0.73	1	0.19	0
Cyclic protocol				
7.2 $\mu\text{m/s}$	0.26	1	-0.19	1
4.3 $\mu\text{m/s}$	0.34	1	-0.18	0
1.35 $\mu\text{m/s}$	0.42	1	-0.10	0

¹ 1=Dependent 0=Independent